Microbial biomarkers support organic carbon transport from methane-rich Amazon wetlands to the shelf and deep sea fan during recent and glacial climate conditions

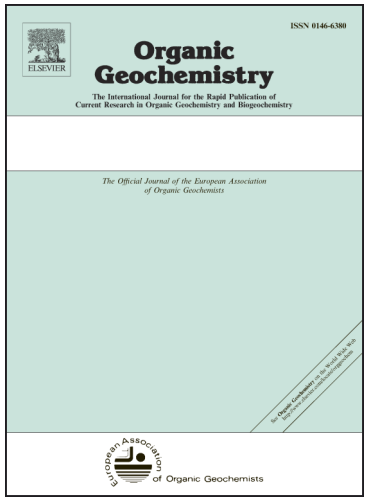

Microbial biomarkers support organic carbon transport from methane-rich Amazon wetlands to the shelf and deep sea fan during recent and glacial climate conditions

Thomas Wagner, Wiebke Kallweit, Helen M. Talbot, Gesine Mollenhauer, Arnoud Boom, Matthias Zabel

PII: S0146-6380(13)00271-4
DOI: http://dx.doi.org/10.1016/j.orggeochem.2013.12.003
Reference: OG 3050

To appear in: *Organic Geochemistry*

Received Date: 21 June 2013
Revised Date: 5 December 2013
Accepted Date: 9 December 2013

Please cite this article as: Wagner, T., Kallweit, W., Talbot, H.M., Mollenhauer, G., Boom, A., Zabel, M., Microbial biomarkers support organic carbon transport from methane-rich Amazon wetlands to the shelf and deep sea fan during recent and glacial climate conditions, *Organic Geochemistry* (2013), doi: http://dx.doi.org/10.1016/j.orggeochem.2013.12.003

Microbial biomarkers support organic carbon transport from methane-rich Amazon wetlands to the shelf and deep sea fan during recent and glacial climate conditions

Thomas Wagner[a,*,Thomas.wagner@ncl.ac.uk], Wiebke Kallweit[e], Helen M. Talbot[a], Gesine Mollenhauer[c], Arnoud Boom[d], Matthias Zabel[b]

[a]School of Civil Engineering and Geosciences, Newcastle University, Drummond Building, Newcastle upon Tyne, NE1 7RU, UK

[b]MARUM – Center for Marine Environmental Sciences, University of Bremen, P.O. Box 330440, 28334 Bremen, Germany

[c]Alfred-Wegener Institute for Polar and Marine Research, Am Handelshafen 12, 27570 Bremerhaven, Germany

[d]Department of Geography, University of Leicester, Bennett Building, Leicester, LE1 7RH, UK

[e]Department of Geosciences, University of Bremen, P.O. Box 330440, 28334 Bremen, Germany

[*]Corresponding author. Tel.: +44 191 222 7893; fax: +44 191 208 5322.

Abstract

We have investigated the delivery of terrestrial organic carbon (OC) to the Amazon shelf and deep sea fan based on soil marker bacteriohopanepolyols (BHPs; adenosylhopane and related compounds) and branched glycerol dialkyl glycerol tetraethers (GDGTs), as well as on ^{14}C dating of bulk organic matter. The microbial biomarker records show persistent burial of terrestrial OC, evidenced by almost constant and high BIT values (0.6) and soil marker BHP concentration [80-230 µg/g TOC (total OC)] on the late Holocene shelf and even higher BIT values (0.8-0.9), but lower and more variable soil-marker BHP concentration (40-100 µg/g TOC) on the past glacial deep sea fan. Radiocarbon data show that OC on the shelf is 3-4 kyr older than corresponding bivalve shells, emphasizing the presence of old carbon in this setting.

We observe comparable and unexpectedly invariant BHP composition in both marine sediment records, with a remarkably high relative abundance of C-35 amino BHPs including compounds specific for aerobic methane oxidation on the shelf (avg. 50% of all BHPs) and the fan (avg. 40%). Notably, these marine BHP signatures are strikingly similar to those of a methane-producing floodplain area in one of the Amazonian wetland (várzea) regions. The observation indicates that BHPs in the marine sediments may have initially been produced within wetland regions of the Amazon basin and may therefore document persistent export from terrestrial wetland regions, with subsequent re-working in the marine environment, both during recent and past glacial climate conditions.

Keywords

Bacteriohopanepolyols; GDGTs; Amazon River and fan; soil organic carbon; microbial biomarker* terrigenous input; aerobic methane oxidation; old carbon; wetlands

1. Introduction

Large amounts of terrigenous organic carbon (OC) are delivered to the oceans by rivers, but only 33% to 50% or even less is ultimately deposited in marine sediments (e.g. Burdige, 2007; Hedges and Keil, 1995). Continental margin systems are of particular importance for storage of riverine suspended OC (Henrichs and Reeburgh, 1987; Schlünz and Schneider, 2000; Walsh et al., 2008). Where riverine suspended matter is channeled directly to the deep sea, submarine fans develop which transport large amounts of terrigenous material to the deep ocean (e.g. Flood et al., 1995; Ittekkot et al., 1986). The mechanism is of particular importance during past glacial periods when global sea level was low and shelf areas were exposed to widespread erosion (Schlünz et al., 1999; Mollenhauer et al., 2004). Further modification of the terrigenous and marine OC signal comes from reworking and subsequent lateral displacement of fine grained sediments, controlled by strong and variable bottom currents (Inthorn et al., 2006; Mollenhauer et al., 2002), that can lead to large age offsets between organic and inorganic components in marine sediments (e.g. Mollenhauer et al.,

2003, 2005; Ohkouchi *et al.*, 2002). The Amazon shelf and fan region is one area where intense sediment reworking, coupled with enhanced degradation of refractory OC has been reported (see reviews for broader context by Aller, 1998; Burdige, 2007).

On the Amazon shelf and deep sea fan, sedimentary OC is dominated by terrigenous material (Boot et al., 2006; Hinrichs and Rullkötter, 1997), derived mainly from soil (Aller et al., 1986; Hedges et al., 1986). Sub-surface soil layers in the Amazon Basin have been shown to have relatively old radiocarbon ages, of the order of several 10^3 yr at <1 m depth (Martinelli et al., 1996; Pessenda et al., 1998, 2001, 2010 and references therein). Additionally, pre-ageing of the OC during temporary storage on floodplains and in lakes, a common process in the Amazon Basin, has been reported (Raymond and Bauer, 2001 Blair *et al.*, 2004).

The Amazon floodplain is a complex system of seasonally flooded forest, lakes and wetlands that covers ca. 800,000 km^2, or 14% of the Amazon basin (Melack and Hess, 2010). Using remote sensing data, Melack and Hess (2010) performed a comprehensive study to provide the areal extent of different subdivisions of the Amazon floodplain, including four subcategories: open water, river channels, flooded forest and aquatic macrophytes, with wetlands covered by aquatic macrophytes and flooded forest accounting for the largest methane emissions in Amazonia.

1.1. Microbial tracers for carbon cycling in soils

A commonly used tool for investigating the supply of soil OC (SOC) to the marine environment is the branched and isoprenoid tetraether index (BIT), which compares relative contributions of predominantly terrestrially derived branched tetraethers to the marine-derived isoprenoid tetraether crenarchaeol (Hopmans et al., 2004). BIT values for soil vary between 0.9 and 1 due to low amounts of crenarchaeol (Weijers et al., 2006) and the approach has been applied in a number of recent studies (e.g. Walsh et al., 2008; Weijers et al., 2009; Zhu et al., 2011a; Kim et al., 2012; Zell et al., 2013). A comprehensive review and the structures of GDGTs is ggiven by Schouten et al. (2013).

Another group of lipid biomarkers with potential for tracing SOC delivery to the marine environment are specific bacteriohopanepolyols (BHPs; pentacyclic triterpenoids produced by a wide range of prokaryotes, e.g. Ourisson et al., 1987; Rohmer et al., 1984; Farrimond et al., 1998; Talbot and Farrimond, 2007). These compounds show a diverse range of structural variation, differing in the number and nature of the functional groups in an extended side chain (Table 1, see Appendix for structures; e.g. Talbot and Farrimond, 2007). Recent studies have demonstrated that adenosylhopane (**Ia**)) is a likely precursor for all other side chain-extended biohopanoids (Bradley et al., 2010). It has also been shown that adenosylhopane and several related compounds, including homologues methylated at C-2 are common and abundant components of soil (**Ia, IIa, Ib, IIb, Ib'** and **IIb'**, Table 1; e.g. Cooke et al., 2008a; Xu et al., 2009; Kim et al., 2011; Rethemeyer et al., 2010) suggesting an additional role for this type of structure besides that of a simple intermediate. These structures are rare in open marine settings (Blumenberg et al., 2010; Zhu et al., 2011b;

Berndmeyer et al., 2013) and have therefore been used to track SOC transport to aquatic environments (Cooke et al., 2008b, 2009; Handley et al., 2010; Zhu et al., 2011b; Sáenz et al., 2011). Zhu et al. (2011b) recently proposed a potential novel proxy (R_{soil}) for tracing SOC in marine sediments by comparing the concentration of "soil marker" BHPs (adenosylhopane and related structures) to the combined bacteriohopane-32,33,34,35-tetrol (BHT) plus total soil marker BHPs. It should be noted, however, that for these purposes BHT can only be considered to be a pseudo marine end member as it is also found in soils, peat and lake sediments (e.g. Talbot and Farrimond, 2007; Cooke et al., 2008a; Rethemeyer et al., 2010; Kim et al., 2011; van Winden et al., 2012), although typically in much lower relative abundance than in marine systems (Blumenberg et al., 2010; Zhu et al., 2011b; Berndmeyer et al., 2013). Recent studies have shown some correlation of the R_{soil} index with both BIT values and bulk $\delta^{13}C$ values in sediments from a Yangtze River-East China Sea transect and a Kalix River transect (Zhu et al., 2011b; Doğrul Selver et al., 2012), supporting its application as an indicator of bacterially-derived SOC.

To identify other important microbial processes within soil environments, we also studied the entire range of BHPs extracted from the sediments, with emphasis on those diagnostic for microbes performing aerobic methane oxidation. Methanotrophs produce highly characteristic BHPs, specifically the 35-aminobacteriohopanepolyols (see Appendix) with three, four or five additional OH groups in the side chain. Type I methanotrophs typically produce penta- and hexafunctionalized structures, with 35-aminobacteriohopane-30,31,32,33,34-pentol (aminopentol; **Ic**) the most diagnostic (Cvejic et al., 2000;

van Winden et al., 2012). The pentafunctionalized 35-aminobacteriohopane-31,32,33,34-tetrol (aminotetrol; **Id**) is produced by all Type I and II methanotrophs (e.g. van Winden et al., 2012 and references therein), but was also detected as a minor component in some strains of sulfate reducing bacteria of the genus *Desulfovibrio* (Blumenberg et al., 2006, 2009, 2012). Aminopentol has also recently been found in trace amount in one species of *Desulfovibrio*, but in this organism, as in all other *Desulfovibrio* spp. shown to be hopanoid producers, the dominant BHPs were the tetrafunctionalized compounds bacteriohopane-32,33,34,35-tetrol (BHT; **If**) and 35-aminobacteriohopanetriol (**Ie**; Blumenberg et al., 2006; 2009; 2012).

1.2. Scope of the study

We present BIT, BHP and ^{14}C data from two sediment cores from the Amazon shelf (GeoB3918) and deep sea fan (GeoB1514) (Fig. 1a), to investigate the relative importance of SOC in these marine sediments covering the most recent interglacial (probably <1000 ka) and past glacial/early deglacial climatic conditions. For comparison we also present sedimentary floodplain and soil derived biomarkers from the interior of the Amazon system (Fig.1b).

2. Material and methods

2.1. Study area and sampling

With an annual sediment discharge of 1.2 x 10^9 tons, the Amazon River is an important source of suspended terrigenous matter in the ocean (Meybeck and

Ragu, 1996). Oceanographic conditions linking Amazon outflow with shallow currents along the Amazon Shelf and upper continental margin have been summarized for modern conditions by Geyer et al. (1991) and for past glacial conditions by Wilson et al. (2011). In short, during Quaternary interglacials with high sea level, suspended terrigenous matter from the Amazon is transported primarily northwestward along the innermost shelf by the North Brazil Coastal Current and deposited on the shelf. During glacial periods, large parts of the current shelf area were exposed and the suspended material from the river was directly channeled through canyons and deposited on the deep Amazon Fan (Milliman et al., 1975), strongly increasing the OC content of glacial sediments (Keil et al., 1997; Schlünz et al., 1999; Burdige, 2005). The far field effects of these temporal changes in outflow and oceanography from the Amazon and Orinoco river regions with regard to OC supply and burial in the southern Caribbean have been discussed by Schlünz et al. (2000).

We analyzed two gravity cores from a shallow and a deep water setting. The sampling site of GeoB3918-2 is on the Amazon shelf at a water depth of 50 m (3.7050°N; 50.4050°W), the core was taken during Meteor cruise M34/4 (Fischer et al., 1996). The region is prone to intense bottom water current activity and sediment reworking under modern climate conditions (Kuehl et al., 1986; Kineke et al., 1996). Core GeoB1514-6 was taken from the deep sea fan at a water depth of 3509 m (5.1383°N; 46.5750°W, Fig. 1a) during Meteor cruise M16/2 (Schulz et al., 1991). Following collection of the sediments they were stored at -20 °C in the core repository in Bremen. Samples were taken at ca. 20 cm (GeoB3918; 27 samples) and 25 cm (GeoB1514; 30 samples)

intervals. All geochemical data refer to the core specified above, except for TOC content for GeoB1514, which was obtained from the sister core GeoB1514-7, as studied by Schlünz (1998) and Schlünz et al. (1999).

In order to investigate the BHP composition from a range of typical soil and sediments from the interior of the Amazonian basin, six locations with different proximity to the Amazon River were sampled near the Colombian town of Puerto Nariño (Fig. 1b, Table 2). The area is characterized by Amazon floodplain (várzea) and high ground (terra firme*)* environments (Forero et al., 2002).

Site 1 represents an open wetland environment dominated by *Montrichardia* macrophytes. The ecosystem covers an abandoned channel and is inundated by the Amazon River on a seasonal basis. Sites 2 - 4 are permanently inundated abandoned channels, covered by open water and surrounded by várzea forests. Site 2 has a minor but permanent connection with the Amazon River. Site 3 is a remnant of an ancient channel from the Amazon River, receiving its water from the surrounding forest and draining into the Loretoyacu River. At high water, Site 3 is flooded from the surrounding várzea. Site 4 is a small old oxbow lake on the Loretoyacu River; it is so distant from the Amazon River that it is flooded from the Loretoyacu alone during high water. The Loretoyacu River is an Amazonian river, draining the nearby terra firme forest on Miocene sediments from the northern part of the Loreto provence in Peru. Located within the terra firme of the Loretoyacu River this lake is not a typical várzea ecosystem. The sample from Site 5 is a soil from an island in the main

Amazon channel; it consists of recent Quaternary Amazon wetland sediments. At maximum flood height, the site is flooded for a short period and the area is used for traditional crop cultivation. Site 6 is a soil from a traditional agricultural plot on top of Miocene sediments in the terra firme.

2.2. Bulk parameters

Accelerator mass spectrometry (AMS) radiocarbon dating of TOC samples was conducted at the National Ocean Sciences Accelerator Mass Spectrometry (NOSAMS) Facility at Woods Hole Oceanographic Institution (USA) on 3 and 4 samples of TOC from cores GeoB3918 and GeoB1514, respectively (Table 3). AMS radiocarbon ages of two bivalve shells from core GeoB3918 measured at the Leibniz laboratory AMS facility at Kiel (H. Arz, personal communication) were converted to calendar years using the CALIB 6.0 algorithm (Stuiver et al., 2010) and the Marine09 data set (Reimer et al., 2009). However, the ^{14}Cage values of TOC were not calibrated, as the Marine09 data set (Reimer et al., 2009) was not suitable, given the high amount of terrigenous material in these samples which could not be determined.

The TOC content for GeoB3918 was measured with a LECO CS-300 elemental analyzer. Two subsamples (60-70 mg) from each sampling depth were filled into ceramic containers, repeatedly treated with 0.25 N HCl until quantitative removal of $CaCO_3$ followed by rinsing with distilled water, and drying at 50 °C for 24 h prior to analysis. After calibration of the analyser with two pure carbon standards (2.48% C +/- 0.02 and 0.064% C), all samples were burned within the

LECO furnace at 2200 °C. An additional standard was measured every 10 samples. Reproducibility was ±5%.

2.3. Extraction and derivatization

2.3.1. GDGTs

Freeze-dried, homogenized sediment (ca. 5 g) was extracted with 25 ml MeOH, dichloromethane (DCM):MeOH (1:1, v/v) and DCM, respectively. Each addition of solvent was followed by 5 min sonication and 5 min centrifugation. A known amount of a C_{46}-GDGT was added as internal standard before extraction. The total lipid extract (TLE) was combined, washed with twice distilled water (Seralpure) to remove salts, dried over anhydrous Na_2SO_4 and concentrated under N_2. The extract was then dissolved in DCM and desulfurized using a Pasteur pipette filled with activated and solvent rinsed Cu filaments (HCl, H_2O, MeOH, DCM). The TLE sample was placed on the column via elution with 4 ml DCM before drying under N_2. It was separated into three polarity fractions using SiO_2 column chromatography (60 mesh, deactviated with 1% wt. H_2O) and elution with 2 ml *n*-hexane (hydrocarbons), 2 ml DCM:*n*-hexane (2:1, v/v, ketones) and 2 ml MeOH (alcohols including GDGTs; Kallweit et al., 2012).

Half of the MeOH fraction was dried, weighed, dissolved in DCM and filtered through a 0.45 µm syringe filter (Whatman). The solvent was evaporated under N_2 and lipids were dissolved in *n*-hexane:isopropanol (99:1, v/v) to a

concentration of 2 mg/ml (Schouten et al., 2009) for high performance liquid chromatography (HPLC) measurement.

2.3.2. BHPs

The extraction method was based on the Kates (1975) modification of the original Bligh and Dyer (Bligh and Dyer, 1959; Kates, 1975) method. The procedure has been described in detail by Cooke et al. (2008a), except for the use of DCM instead of $CHCl_3$. After addition of the internal standard (5α pregnane-3β20βdiol) the sample was acetylated (2 ml pyridine, 2 ml Ac_2O for 1 h at 50 °C and left at room temperature overnight. The sample was evaporated to dryness under N_2, dissolved in MeOH/propan-2-ol (60:40, v/v) and filtered through a 0.45 µm PTFE syringe filter. For HPLC-tandem mass spectrometry ($LC\text{-}MS^n$), the extract was dried again under N_2 and dissolved in a defined volume (500 µl) of MeOH/propan-2-ol (60:40, v/v).

2.4. Chromatography

2.4.1. Analytical HPLC-APCI-MS for GDGT measurement

GDGTs were measured using normal phase HPLC with an Agilent 1200 series HPLC system and Agilent 6120 single-quadrupole MS instrument under atmospheric pressure chemical ionization (APCI) conditions. Instrumental were given by Leider et al. (2010). GDGT concentration was calculated from the characteristic peak area of $[M+H]^+$ of individual GDGTs relative to that from the

internal standard at *m/z* 744. It should be noted tha, due to the lack of a pure branched GDGT (brGDGT) standard to allow determination of relative response factors (cf. Huguet et al., 2006), concentration values are not absolute, however, relative values are valid. The BIT index, quantifying the relative abundance of brGDGTs with *m/z* 1022, 1036 and 1050 and crenarchaeol (m/z 1292, Hopmans et al., 2004) was calculated from the respective peak areas for the estimation of SOC input to the core locations. Analytical precision was determined by repeated extraction and measurement of a laboratory internal sediment standard and duplicate analysis of selected samples. The analytical error for GDGT quantification was ± 10% and standard deviation of BIT values was < 0.01 unit.

A second index based on relative abundance of the soil-derived brGDGTs, the methylation index of branched tetraethers (MBT), was also calculated according to Weijers et al. (2007). Here, the peak areas of $M^{+\cdot}$ ions at m/z 1018, 1020, 1022, 1032, 1034, 1036, 1046, 1048 and 1050 were determined in a second HPLC-MS analytical run using the same instrument settings as described above for BIT index values.

2.4.2. Analytical HPLC-APCI-MS for BHP measurement

BHPs were measured using reversed-phase HPLC-APCI-MS as described previously (e.g. Cooke et al., 2008a; van Winden et al., 2012). Structures were assigned from comparison with published mass spectra (Rethemeyer et al., 2010; Talbot et al., 2003a,b, 2007a,b, 2008).

A semi-quantitative estimate of abundance (± 20%) was calculated from the characteristic base peak ion areas of individual BHPs in mass chromatograms relative to the *m/z* 345 ($[M+H–CH_3COOH]^+$) base peak area response of the acetylated 5α-pregnane-3β,20β-diol internal standard. Relative response factors for BHT representing non-N containing BHPs and the average of four N-containing BHPs, including aminotriol, adenosylhopane, BHT-cyclitol ether and BHT glucosamine were used to adjust the peak areas relative to that of the internal standard, where BHPs containing one or more N atoms give an averaged response ca. 12 x that of the standard and those with no N give a response 8 times that of the standard (e.g. van Winden et al., 2012). The R_{soil} Index, based on the proportion of soil marker BHP against the pseudo-marine end member bacteriohopanetetrol (BHT, **If**), was calculated according to Zhu et al. (2011b):

$$R_{soil} = [Ia+IIa+Ib+IIb+Ib'+IIb']/[Ia+IIa+Ib+IIb+Ib'+IIb'+If]$$

3. RESULTS

3.1 Radiocarbon data

Radiocarbon dating of GeoB 3918 was conducted on TOC and bivalve shells. Bivalve shells from 3.8 and 4.5 m core depth were dated at 860 ± 40 and 1030 ± 40 ^{14}C yrs BP, respectively, revealing a depositional age of 450 ± 40 and 580 ± 40 cal yr BP. Corresponding ^{14}C dating of three TOC samples gave an older age around 4000 ^{14}C yr BP (Table 3), with internal age reversals, emphasizing

the presence of old carbon and the importance of reworking. Radiocarbon dating on TOC from GeoB 1514 was conducted on four samples from between 0.4 and 6.9 m, producing radiocarbon ages from 13650 to 30200 ^{14}C yr BP (Table 3).

3.2. TOC

TOC concentrations was consistent between 0.6 and 0.7%, on the shelf (GeoB3918; Fig. 2), whilst the profile for GeoB1514 (Fig. 2) from the deep sea fan had a well known trend, with low TOC (0.3%) in the top part, a sharp rise to ca. 0.6% at ca. 0.5 m, and a step at about 5.0 m and then with further gradually increasing values towards the core bottom (Schlünz et al., 1999).

3.3 GDGT concentrations and BIT index

Concentrations of soil-derived brGDGTs (see e.g. Hopmans et al., 2004; Weijers et al., 2007 for GDGT structures) varied between 43.2 and 68.6 µg/g TOC on the shelf (GeoB3918; Table 4) and between 9.6 and 327.9 µg/g TOC in the fan core (GeoB1514; Table 4). Corresponding crenarchaeol concentration ranged from 24.3 to 52.6 µg/g TOC (GeoB3918) and from 6.5 to 77.6 µg/g TOC (GeoB1514), with significant fluctuation, especially in the fan core. The BIT index was high in both cores, fluctuating between ca. 0.5 to 0.6 in GeoB3918 (Fig. 2) and reaching values around ca. 0.8 to 0.9 in GeoB1514 (Fig. 2). Lower

BIT values in the upper section of both cores, reaching ca. 0.5 near the sediment surface, documented reduced supply of SOC.

3.4. BHP composition

Up to 21 BHPs were identified in samples from GeoB1514 (Table 5) and up to 18 of these were also observed in GeoB3918; Table 6). Total concentration ranged from 1124 to 2863 µg/g TOC (GeoB3918; Fig. 2a, Table 6) and 109 to 2513 µg/g TOC (GeoB1514; Fig. 2, Table 5).

Soil marker BHPs (e.g. Cooke et al., 2008a,b; Rethemeyer et al., 2010; Tables 5 and 6) comprising adenosylhopane (**Ia**), its C-2 methylated homologue (**IIa**) and up to four related structures with different terminal groups located at C-35 (**Ib, IIb, Ib'** and **IIb'; Table 1**) were found in all samples, with the exception of the 10 cm sample from GeoB1514. The concentration wass higher on the shelf (mean 149 µg/g TOC, SD 45, range 77-222 µg/g TOC; Fig. 2, Table 6) and generally lower (mean 59 µg/g TOC, SD 45, range 4-166 µg/g TOC) on the fan (excluding the 2 Holocene surface samples; Fig, 2, Table 5). The corresponding relative proportion of soil marker BHPs was low, ranging from 6-15% (GeoB3918; Fig. 2a, Table 6) and 1-12% (GeoB1514; Table 5). Consistent with a late Holocene setting, the concentration of soil marker BHPs was low or below detection in the uppermost section of GeoB1514. R_{soil} index values (Zhu et al., 2011b) varied between both cores (Fig. 2), with generally higher values between 0.21 and 0.31 (avg. 0.26, standard deviation [SD] 0.03) on the shelf

and more variable values on the deep sea fan (range 0-0.39, av. 0.17, SD 0.09; Table 4).

A suite of compounds linked to aerobic methane oxidizing bacteria, including aminobacteriohopanetetrol (aminotetrol, **Id**) and aminobacteriohopanepentol (aminopentol, **Ic**) as well as a related isomer (**Ic'**) and unsaturated aminopentol (**III** or **IVc,** respectively; van Winden et al., 2012 and references therein) was identified in all samples. Collectively we termed this group of compounds "CH_4 oxidation markers". In addition to these diagnostic structures, we also observed a high concentration of the related aminotriol (**Ie**) together with an unsaturated homologue (**IIIe**), although the position of the unsaturation could not be confirmed but could be in the side chain (cf. van Winden et al., 2012). However, we excluded the latter two compounds from the "CH_4 oxidatio -markers" group as they can be derived from other sources besides methanotrophs (e.g. Talbot and Farrimond, 2007; Talbot et al., 2008).

Methane oxidation markers constituted on average 36% of the total BHPs (SD, 3.9%) in the shallow shelf core GeoB3918 (Fig. 3a). Similarly invariant, but lower (18%, SD 4.9%) average relative proportions of methane oxidation markers were recorded in GeoB1514 (Fig. 3b). The relative contribution of aminotriol, another potential but not exclusive marker for aerobic methane oxidation (e.g. van Winden et al., 2012), was similar in both cores, adding on average another 19-21% to the total BHP pool. Combined, 40-60% of all BHPs were potentially derived from aerobic methane oxidizers (Fig. 3).

In addition to these two main groups of compounds and the aminotriols, a suite of "other-BHPs" (See Tables 2, 5 and 6 for all structures in this group) were also detected, including the commonly occurring BHT (**If**) and its C-2 methylated homologue 2-MeBHT (**IIf**). Several composite BHPs (i.e. with a more complex group at C-35, such as a sugar or amino sugar) were observed, but they could not be assigned to any particular group of source organisms (Table 1), so are not further discussed in detail. In all samples this "other–BHPs" group was dominated by the tetrafunctionalized compound, BHT cyclitol ether (**Ih**), containing an amino sugar moiety at C-35, in most cases, with lower relative proportions of both the penta- and hexafunctionalized homologues (**Ih** and **Ij** respectively), together with low levels of some C-2 methylated homologues (**IIi** and **IIj**). Interestingly, the relative proportions of each group of compounds remained roughly constant with depth, despite large variation in concentration, particularly in core GeoB3918 (Figs. 2, 3; Tables 5, 6).

3.5. BHP composition in Amazonian wetland and forest soils

The relative distribution of BHPs in the Amazonian wetland sediments and soil samples was more diverse than in the marine sediments (Fig. 4, Table 2). The samples, however, contained all of the compounds observed in the shelf and fan sediments, with the exception of one methylated soil marker compound (**IIb'**), which is a minor compound in GeoB3918 (Table 5) and frequently absent from GeoB1514 (Table 6). Using the same compound grouping as for the marine cores, the comparison of the relative proportions of CH_4 oxidation

markers, aminotriol, soil marker BHPs and other BHPs showed remarkable similarity between the wetland and forest samples (sites 1-3) and the marine deposits. This especially held for the high relative contribution of methane oxidation markers (avg. 36.7%) and aminotriol (avg. 23.5%). In contrast to Sites 1-3, Site 4 is not a typical várzea setting and contained considerably lower concentrations of the methane oxidation marker BHPs. This was also observed in the soil samples from Sites 5-6 (Fig. 1 and 4), at which the methane oxidation biomarkers comprised < 20% of the total BHPs. As anticipated, the proportion of soil marker BHPs were elevated in the soil samples and also at Site 4, between 17.5 and 27.6%, but strongly decreased to 2.6-11.2% in the typical várzea wetland sediments (Sites 1-3). R_{soil} values varied considerably, even between the two soils (0.44 Site 5 and 0.84 site 6).

4. Discussion

4.1 Limitations on stratigraphic control

Sediments from the shelf core GeoB3918 were deposited during the most recent part of the Holocene, as suggested from the ^{14}C data (Table 3). Further refinement of specific ages at certain depths was not possible and is beyond the scope of the study, emphasizing the homogenized nature of the core material, which is likely related to intense and widespread reworking of sediment along the Amazon shelf (Aller, 1998; Burdige, 2007).

No carbonate based radiocarbon chronology exists for GeoB1514. Therefore, the age assignment of this core must rely on correlation with the record from the nearby ODP site 942, for which a reliable radiocarbon based age model has been established (Bendle et al., 2010). We use the MBT index record of GeoB1514 for correlation with the published record from ODP site 942, as both show a distinct pattern of variability that is consistent across both cores (Fig. 5). Based on this alignment, the bottom of core GeoB1514 is probably ca. 36500 yr old, while the top has an approximate age of slightly < 10000 yr, barely reaching the Holocene. The uppermost ca. 30 cm of GeoB1514 have been described as consisting of calcareous clay, separated from the underlying clay by an iron rich crust, as often described from the Amazon Fan (e.g. Damuth and Flood, 1984). Similar depth changes in lithology and TOC concentration have been reported from various cores from the region (Debrabant and Chamley, 1997; Schlünz et al., 1999 and references therein) and support an early Holocene age for the uppermost core section. It must be noted, however, that our alignment only results in a coarse age determination of core GeoB1514, which inevitably is associated with large uncertainty. Therefore, we only make qualitative estimates with regard to the age structure of the sediments deposited at the site. We distinguish between sections deposited during glacial conditions, with low sea level (below about 30 cm) and those deposited during the early deglacial sea level rose above ca.30 sediment depth.

4.2 Tracing soil organic matter using molecular and isotopic proxy data

SOC is a prominent constituent of sediments from the Amazon shelf and fan, but its relative importance is not easy to determine from bulk $^{13}C_{org}$, BIT, soilmarker BHP concentration and R_{soil} index. Previous estimates based on bulk carbon isotopes suggest that terrigenous OC makes up 60-90% of the TOC in the glacial sediments in GeoB1514 (Schlünz, 1998), consistent with high BIT values between 0.50 and 0.92 obtained here. This good match of two independent lines of evidence builds confidence in our ability to estimate relative contributions of terrigenous sedimentary organic matter in marine sediments, at least in deep sea fan settings with prominent supply from C_3 plant vegetation. Notably, the range of BIT values from GeoB1514 is comparable with those reported for suspended particulate matter (0.41-0.92) and riverbed sediments (0.89-0.94) from the Amazon catchment (Kim et al., 2012; Zell et al., 2013).

Direct comparison of these BIT and δ^{13}Corg results with soil marker BHP concentration and R_{soil} index from Amazon deep sea fan sediments is not easy and any correlation is likely to vary with local end members (Zhu et al., 2011b). Recently, it has been shown that soil marker BHPs and associated R_{soil} values are attenuated more rapidly than the brGDGTs and BIT values in a modern Yangtze River-East China Sea surface sediment transect (Zhu et al., 2013). These observations were ascribed to possible preferential settling of BHPs near shore and in situ production of brGDGTs, emphasizing the different behavior of both microbial biomarker groups as they travel from their continental source to their final marine sink, as well as uncertainty in marine BHP end member

signatures (as BHT can have both marine and terrestrial sources; Zhu et al., 2011b).

Concentrations of soil marker BHP on the shelf (Fig. 2, Table 5) is generally high compared with other marine studies (Blumenberg et al., 2010; Zhu et al., 2011b) and shows the expected enrichment on the shelf. In contrast, values for the fan sediments are somewhat lower and similar to those reported from the Congo deep sea fan covering the last 34 ka (23-120 µg/gTOC; Handley et al., 2010). The gradually decreasing R_{soil} values are consistent with the decreasing trend in soil marker BHP concentration between the shelf and deeper slope/fan setting. Observations from surface sediment transects from the modern Yangtze River-East China Sea (Zhu et al., 2011b) and the Kalix River (Droğul Selver et al., 2013) have found correlation between R_{soil}, BIT and $\delta^{13}C$ values. In our study, however, we do not observe any clear correlation between R_{soil} and BIT index down core (Fig. 6), consistent with observations from the Tête River in the Gulf of Lyons (Kim et al., 2011). We suggest that the observed mismatch between BIT and the BHP and $\delta^{13}C$ proxies results at least partly from in situ production of brGDGTs in the sediments (e.g. Peters et al., 2009; Zhu et al., 2011b; Zell et al., 2013), however, at this point there is no evidence to discuss this further. Taken together, the evidence strongly argues that each different depositional system requires its own individual proxy calibration.

The ^{14}C age of OC is much older than that of bivalve shells on the shelf (GeoB3918, Table 3). Likewise, the bulk OC ^{14}C ages of GeoB1514 from the fan are up to about 4000 ^{14}C yr older than for the corresponding bivalve shell. This observation is consistent with the presence of old OC in the area (Kuehl et

al., 1986; Sommerfield et al., 1995) and supports the concept that part of the OC is derived from pre-aged terrestrial (including soil) OC, either from the catchment and/or from erosion of exposed older strata on the shelf during periods of sea level low stand and/or transgression. Based on the current evidence we cannot distinguish between the two processes. We suggest, however, that the observed old ^{14}C ages and biomarker signatures in the Amazon fan sediments result from export and/or mobilization of pre-aged terrigenous (possibly soil-derived) OC, either from the Amazon catchment itself and/or from older (relict) sediments exposed along the shelf. The latter is known to be influenced by strong bottom currents, producing widespread lag deposits (Fischer et al., 1996), at least under modern climate conditions.

4.3. Potential sources for aerobic methane oxidation signatures

Amino BHPs, with the exception of the aminotriol (**Ie**), are an important group in the samples, and which are generally considered to be specific for aerobic methane oxidation. Indeed 40-50% of all BHPs in the core samples are potentially derived from aerobic methane oxidizers ("CH_4 oxidation markers" plus "aminotriols"; Tables 5 and 6; Fig. 3), which is exceptional for any marine sediment where typically only aminotriol occurs (e.g. Ace Lake, marine Unit II sediments, Coolen et al., 2008; Benguela upwelling system, Blumenberg et al., 2010; various other marine upwelling systems, Saénz et al., 2011; East China Sea, Zhu et al., 2011b). However, traces of aminotetrol and occasionally aminopentol have been observed in some Arctic shelf sediments (Cooke et al.,

2009; Taylor and Harvey, 2011). Such high values as observed here are more typical for lake sediments, where high relative proportions of aminotriol, together with large contributions of aminotetrol and aminopentol (total > 40%), have been reported (Talbot et al., 2003c; Talbot and Farrimond 2007; Coolen et al., 2008).

Several potential sources need to be considered for these diagnostic BHPs, including (i) marine sources, (ii) soils and (iii) other methane-producing sub-settings in the river catchment.

4.3.1. Marine sources

In situ production of amino BHPs within the near surface shelf and fan sediments does not seem likely since the major organisms that produce these compounds are aerobes (e.g. van Winden et al., 2012 and references therein). It has been shown that fan sediments become anoxic at 20 to 30 cm below the sediment surface (Schulz et al., 1994). Furthermore, porewater data from site GeoB3918 show a high mineralization rate on the shelf, with a shallow oxic surface layer and anoxic conditions below 12 cm sediment depth (Fischer et al., 1996). Finally, SO_4^{2-} is entirely depleted in ca. 1 m sediment depth, arguing against a marine origin of the biomarker signal since the only alternative known sources are some species of sulfate reducing bacteria of the genus *Desulfovibrio,* some of which have been found (Blumenberg et al., 2006, 2009, 2012) to produce aminotetrol (**Id**) and most recently aminopentol (**Ic**), both only in trace quantities relative to the dominant aminotriol (**Ie**) and BHT (**If**). We

recognize that the exceptionally high concentration of hexafunctionalized compounds, particularly aminopentol (**If**, Table 5, 6) in both cores is uncommon for marine sediments. This is because the dominance of sulfate reduction at and near the sediment surface, at least under modern conditions, efficiently limits or prevents the release of methane to the active benthic boundary layer and the water column (see summary byJørgensen and Kasten, 2006). Despite evidence for the presence of methane in Amazon shelf (Figueiredo et al., 1996) and fan sediments (Flood et al., 1995; Shipboard Scientific Party, 1995), it therefore seems highly unlikely that free methane escapes, or has escaped, into the oxic parts of the sediments (Barnes and Goldberg, 1976; Blair and Aller, 1995) to stimulate and sustain the presence of methanotrophs, which in theory could have produced strong and consistent amino BHP signatures in the marine sediments.

4.3.2. Soil biomarker sources

Another possible source of the amino BHPs is microbial organisms in soils. Soil samples have been shown to contain a highly diverse BHP composition (e.g. Cooke et al., 2008b; Xu et al., 2009; Cooke, 2010; Rethemeyer et al., 2010; Kim et al., 2011). Aminopentol (**Ic**) and related compounds (methylated or unsaturated homologues) were, however, only rarely present and never abundant in any of the soils analyzed. It must be noted, though, that the current database on BHP composition in tropical soils and river sediments is in its

infancy, making any judgment preliminary. Still, based on the information available, soil is an unlikely source for the compounds found in this study.

4.3.3. Wetland sources

Another continental sub-setting characterized by high methane production is wetlands. Extensive areas of floodplain and other permanently or seasonally flooded wetlands are well known in the Amazon Basin (e.g. Dunne et al., 1998; Räsänen et al., 1991; Melack et al., 2004). Optical and microwave remote sensing systems, including synthetic aperture radar (SAR), has recently been applied to map the extent and distribution of Amazonian wetlands (Melack and Hess, 2010). Accordingly, the total floodable area within the Amazon lowland (< 500 m above sea level), comprising Amazonian wetlands and other regions that are temporarily flooded, is ca. 800,000 km^2, or 14% of the entire Amazon basin. Melack and Hess (2010), however, stress that the actual floodable area is likely to be even larger, since high altitude wetlands and floodplains in the SW Amazon and the numerous low order streams, as well as small inter-fluvial wetlands, are not well delineated with SAR. Still, the remote sensing study emphasizes the wide distribution of floodplain and wetland areas along the main stem of the Amazon, accounting for 12% of the lowland basin's wetlands, with ca. 75% covered by forest, woodland or shrubland. The striking similarity between the BHP composition in both marine cores and the floodplain deposits (Figs. 3 and 4, Sites 1-3) may therefore suggest that the BHP biomarkers in both marine records could have been produced within a similar Amazonian

floodplain or wetland varzea environment, but not necessarily at the specific location studied.

4.3.4. Depositional processes

Our data from the Puerto Nariño region support the concept that Amazonian wetland environments are capable of producing substantial amounts of amino BHPs and probably also soil BHPs and brGDGTs, which are partly preserved in the sediments. However, we are unable within the scope of the study to further narrow down potential wetland areas in the catchment, which may have served as sources for BHPs transported to the shelf and deep sea fan.

We consider that erosion and downstream transport of sediment and suspended material from wetland environments, possibly combined with intermittent storage of riverine particulate material in sedimentary pools further downstream, may result in accumulation of wetland material close to the river mouth. This material could be exported to the Amazon shelf preferentially during wet periods (seasonal and longer term), where it would be diverted with the prevalent shallow current system during Holocene high sea level, or more directly channeled to the deep sea fan during glacial periods of low sea level. This general concept seems to be supported by observations from the main stem of the Amazon River, which emphasize that OM across the river catchment is surprisingly homogenous (Devol and Hedges, 2001). This homogeneity arises from the large variability in vegetation and soil type within the Amazon system. A further additional contribution arises from the presence

of refractory and older carbon that is aged before being mobilized and/or temporarily stored, along with young carbon at upstream sites. More recent geochemical studies (e.g. Moreira-Turcq et al., 2003) and process-based modelling (Bustillo et al., 2010) are consistent with these observations, also emphasizing the role of wetlands and floodplains as important environments for OC production and export.

We propose that the dominant process that modifies the export signal from the Amazon River is current induced reworking of sediment material on the modern shelf and/or during transport to the deep sea fan during low sea level. The process is known to be highly efficient under modern conditions (Kuehl et al., 1986; Druffel et al., 2005) and, by analogy, during past warm periods with high sea level, leading to widespread areas where older strata were exposed to strong currents on the shallow shelf. Consistent with these processes, the region around GeoB3918 is dominated by lag deposits (Fischer et al., 1996). We consequently consider that any biomarker (and other) component exported from the river catchment to the inner shelf will be strongly affected by these dynamic sedimentary controls, to result in a rather homogenous sediment composition, both on the shelf and the deeper fan. The observed almost constant BIT index value and the low proportion of soil BHPs relative to total BHPs in our records is consistent with this interpretation.

5. Conclusions

This study presents combined microbial biomarker and ^{14}C records from recent shelf and glacial deep sea fan deposits from the Amazon, emphasizing the potential importance of OC export from wetland environments to marine sediments.

The strikingly constant and high contribution of amino BHPs, compounds indicative of aerobic oxidation of methane, relative to total BHPs in the sediments (50% on the shelf, 40% on the fan) and elevated BIT values (0.6 on the shelf, 0.8-0.9 on the fan) argues for a common, terrestrial source. The strong similarity in BHP composition in the marine cores with those in Amazonian floodplain lake samples support the idea that high methane producing environments are the origin of the BHP signatures. These observations potentially identify a new molecular marker to trace the supply from continental wetlands to the ocean, supporting the concept that reworked and old OC from the continent can impose a major influence on the molecular signatures of marine sediments.

More detailed work is required to better constrain the variability in microbial organic signatures in the different sub-environments of river catchments and their pathways and residence times during transport to the ocean. This should include an assessment of how representative geochemical signatures from specific depositional settings are in explaining the large variety of catchment-shelf systems with regard to their size and topography, was well as climate zone. Such a more comprehensive approach to modern systems may be extended to studies of global climate change in the past where wetland

dynamics have been proposed as an important component of warm climate conditions (including Quaternary interglacials and hyperthermal events).

Acknowledgments

We thank the anonymous reviewersfor constructive comments. H. Arz is thanked for providing two ^{14}C ages. Thanks go to J. Rethemeyer for assistance during BHP extractions. The technical staff from FB5 and Marum (Bremen) are thanked for support, especially R. Kreutz for assistance during lab work and B. Kockisch for TOC measurements. The study was supported by the DFG International Graduate College EUROPROX. K. Osborne is thanked for technical assistance in preparing the wetland and soil samples (Newcastle). We thank the Science Research Infrastructure Fund (SRIF) from the HEFCE for funding the purchase of a ThermoFinnigan LCQ ion trap mass spectrometer (Newcastle University) and K. Osborne for technical assistance. T.W. acknowledges support from the Royal Society Wolfson Research Merit Award and H.T. acknowledges funding from the European Research Council grant agreement number (258734 - AMOPROX).

Associate Editor – **E.A. Canuel**

References

Aller, R.C., 1998. Mobile deltaic and continental shelf muds as suboxic, fluidized bed reactors. Marine Chemistry 61, 143-155.

Aller, R.C., Mackin, J.E., Cox, R.T., Jr. , 1986. Diagenesis of Fe and S in Amazon inner shelf muds: apparent dominance of Fe reduction and implications for the genesis of ironstones. Continental Shelf Research, 6, 263-289.

Barnes, R.O., Goldberg, E.D., 1976. Methane production and consumption in anoxic marine sediments. Geology 4, 297-300.

Bendle, J. A., Weijers J.W.H., Maslin, M., Sinninghe Damsté, J.S., Schouten, S., Hopmans, E.C., Boot, C.S., Pancost, R.D., 2010. Major changes in glacial and Holocene terrestrial temperatures and sources of organic carbon recorded in the Amazon fan by tetraether lipids. Geochemistry, Geophysics, Geosystems 11, doi:10.1029/2010GC003308.

Blair, N.E., Aller, R.C., 1995. Anaerobic methane oxidation on the Amazon shelf. Geochimica et Cosmochimica Acta, 59, 3707-3715.

Blair, N.E., Leithold, E.L., Aller, R.C., 2004. From bedrock to burial: the evolution of particulate organic carbon across coupled watershed-continental margin systems. Marine Chemistry 92, 141-156.

Bligh, E.G., Dyer, W.J., 1959. A rapid method of total lipid extraction and purification. Canadian Journal of Biochemistry and Physiology 37, 911-917.

Boot, C.S., Ettwein, V.J., Maslin, M.A., Weyhenmeyer, C.E., Pancost, R.D., 2006. A 35,000 year record of terrigenous and marine lipids in Amazon Fan sediments. Organic Geochemistry 37, 208-219.

Berndmeyer, C., Thiel, V., Schmale, O., Blumenberg, M., 2013. Biomarkers for aerobic methanotrophy in the water column of the stratified Gotland Deep (Baltic Sea). Organic Geochemistry 55, 103-111.

Blumenberg, M., Krüger, M., Nauhaus, K., Talbot, H.M., Oppermann, B.I., Seifert, R., Pape, T., Michaelis, W., 2006. Biosynthesis of hopanoids by sulfate-reducing bacteria (genus *Desulfovibrio*). Environmental Microbiology 8, 1220-1227.

Blumenberg, M., Oppermann, B.I., Guyoneaud R., Michaelis, W., 2009. Hopanoid production by *Desulfovibrio bastinii* isolated from oilfield formation water. FEMS Microbiology Letters 293, 73-78.

Blumenberg, M., Mollenhauer, G., Zabel, M., Reimer, A., Thiel, V., 2010. Decoupling of bio- and geohopanoids in sediments of the Benguela Upwelling System (BUS). Organic Geochemistry 41, 1119-1129.

Blumenberg, M., Hoppert, M., Krüger, M., Dreier, A., Thiel, V., 2012. Novel findings on hopanoid occurrences among sulfate reducing bacteria: Is there a direct link to nitrogen fixation? Organic Geochemistry 49, 1-5.

Bradley, A.S., Pearson, A., Sáenz, J.P., Marx, C.J., 2010. Adenosylhopane: The first intermediate in hopanoid side chain biosynthesis. Organic Geochemistry 41, 1075-1081.

Burdige, D.J., 2005. Burial of terrestrial organic matter in marine sediments: A re-assessment. Global Biogeochemical Cycles 19, GB4011, doi: 10.1029/2004gb002368.

Burdige, D.J., 2007. Preservation of organic matter in marine sediments: Controls, mechanisms, and an imbalance in sediment organic carbon budgets? Chemical Reviews 107, 467-485.

Bustillo, V., Luiz Victoria, R., Sousa de Moura, J.M., Victoria, D.D.C., Andrade Toledo, A.M., Colicchio, E., 2011. Biogeochemistry of Carbon in the Amazonian Floodplains over a 2000-km Reach: Insights from a Process-Based Model. Earth Interactions 15, 1-29.

Cvejic, J.H., Bodrossy, L., Kovacs, K.L., Rohmer, M., 2000. Bacterial triterpenoids of the hopane series from the methanotrophic bacteria Methylocaldum spp.: phylogenetic implications and first evidence for an unsaturated aminobacteriohopanepolyol. FEMS Microbiology Letters 182, 361-365.

Cooke, M.P., 2010. The Role of Bacteriohopanepolyols as Biomarkers for Soil Bacterial Communities and Soil Derived Organic Matter. PhD Thesis, Newcastle University, UK.

Cooke, M.P., Talbot, H.M., Farrimond, P., 2008a. Bacterial populations recorded in bacteriohopanepolyol distributions in soils from Northern England. Organic Geochemistry 39, 1347-1358.

Cooke, M.P., Talbot, H.M., Wagner, T., 2008b. Tracking soil organic carbon transport to continental margin sediments using soil-specific hopanoid biomarkers: A case study from the Congo fan (ODP site 1075). Organic Geochemistry 39, 965-971.

Cooke, M.P., van Dongen, B.E., Talbot, H.M., Semiletov, I., Shakhova, N., Guo, L., Gustafson, Ö., 2009. Transport of terrestrial organic matter to the

Arctic Ocean via the great Arctic rivers. Organic Geochemistry 40, 1151-1159.

Coolen M.J.L, Talbot H.M., Abbas, B.A., Ward, C., Schouten, Volkman, J.K., Sinninghe Damsté, J.S., 2008. Sources for sedimentary bacteriohopanepolyols as revealed by 16S rDNA stratigraphy. Environmental Microbiology 10, 1783-1803.

Damuth, J.E., Flood, R.D., 1984. Morphology, sedimentation processes, and growth pattern of the Amazon deep-sea fan. Geo-Marine Letters 3, 109-117.

Debrabant, T., Lopez, M., Chamley, H., 1997. Clay mineral distribution and significance in Quaternary sediments of the Amazon fan In: ????, R.D., F., Piper, D.J.W., Klaus, A., Peterson, L.C. (Eds.), Proceedings of the Ocean Drilling Program, Scientific Results 155. Ocean Drilling Program, College Station, TX, pp. 177-192.

Devol, A.H., Hedges, J.I., 2001. Organic matter and nutrients in the mainstem Amazon River. In: McClain et al. (Eds.), The Biogeochemistry of the Amazon Basin. Oxford University Press, New York, pp. 275-306.

Doğrul Selver, A., Talbot, H.M., Gustafsson, O, Boult, S., van Dongen B.E., 2012. Soil organic matter transport along an sub-Arctic river-sea transect. Organic Geochemistry 51, 63-72.

Druffel, E.R.M., Bauer, J.E., Griffin, S., 2005. Input of particulate organic and dissolved inorganic carbon from the Amazon to the Atlantic Ocean. Geochemistry, Geophysics, Geosystems 6, Q03009.

Dunne, T., Mertes, L.A.K., Meade, R.H., Richey, J.E., Forsberg, B.R., 1998. Exchanges of sediment between the flood plain and channel of the Amazon River in Brazil. Geological Society of America Bulletin 110, 450-467.

Farrimond, P., Fox, P.A., Innes, H.E., Miskin, I.P., Head, I.M., 1998. Bacterial sources of hopanoids in recent sediments: Improving our understanding of ancient hopane biomarkers. Ancient Biomolecules 2, 147-166.

Figueiredo, A.G., Jr., Nittrouer, C.A., Costa, E.D.A., 1996. Gas-charged sediments in the Amazon submarine delta. Geo-Marine Letters 16, 31-35.

Fischer, G., and Shipboard Scientific Party, 1996. Report and preliminary results of METEOR-Cruise M34/4, Recife – Bridgetown, 19.3.-15.4.1996. Berichte, Fachbereich Geowissenschaften, Universität Bremen 80, 105 pp.

Flood, R.D., Piper, D.J.W., Shipboard Scientific Party, 1995. Introduction. In Flood, Piper, D.J.W., Klaus, A., et al. (Eds), Proceedings of the Ocean Drilling Program, Initial Reports, 155. College Station, TX (Ocean Drilling Program), pp.5-16.

Forero, G., Ferreira, P., Maya, M., García, E., Martínez, J.O., Núñez, A., Cardozo, E., Nivia, A., González, H., Cepeda, H., Clavijo, J., 2002. Atlas Geológico Digital de Colombia Versión 1.1 (26 planchas). Escala 1:500.000. INGEOMINAS Bogotá.

Geyer, W.R., Beardsley, R.C., Candela, J., Castro, B.M., Legeckis, R.V., Lentz, S.J., Limeburner, R., Miranda, L.B., Trowbridge, J.H., 1991. The physical Oceanography of the Amazon outflow. Oceanography 4, 8–14.

Handley L., Talbot, H.M., Cooke, M.P., Anderson, K.E., Wagner, T., 2010. Bacteriohopanepolyols as tracers for continental and marine organic matter supply and phases of enhanced nitrogen cycling on the late Quaternary Congo deep sea fan . Organic Geochemistry 41, 910-914.

Hedges, J.I., Clark, W.A., Quay, P.D., Richey, J.E., Devol, A.H., de M. Santos, U., 1986. Compositions and fluxes of particulate organic material in the Amazon River. Limnology and Oceanography 31, 717-738.

Hedges, J.I., Keil, R.G., 1995. Sedimentary organic matter preservation: an assessment and speculative synthesis. Marine Chemistry 49, 81-115.

Henrichs, S.M., Reeburgh, W.S., 1987. Anaerobic mineralisation of marine organic matter: rates and role of anaerobic processes in the oceanic carbon economy. Geomicrobiology Journal 5, 191-237.

Hinrichs, K.-U., Rullkötter, J., 1997. Terrigenous and marine lipids in Amazon Fan sediments: Implications for sedimentological reconstructions. In: Flood, R.D., Piper, D.J.W., Klaus, A., L.C. Peterson, L.C. (Eds.), Proceedings of the Ocean Drilling Program, Scientific Results, 155 College Station, TX (Ocean Drilling Program), pp. 539-553.

Hopmans, E.C., Weijers, J.W.H., Schefuß, E., Herfort, L., Sinninghe Damsté, J.S., Schouten, S., 2004. A novel proxy for terrestrial organic matter in sediments based on branched and isoprenoid tetraether lipids. Earth and Planetary Science Letters 224, 107-116.

Huguet, C., Hopmans, E.C., Febo-Ayala, W., Thompson, D.H., Sinninghe Damste, J.S., Schouten, S. 2006. An improved method to determine the

absolute abundance of glycerol dibiphytanyl glycerol tetraether lipids. Organic Geochemistry 37, 1036–1041.

Inthorn, M., Wagner, T., Scheeder, G., Zabel, M., 2006. Lateral transport controls distribution, quality, and burial of organic matter along continental slopes in high-productivity areas. Geology 34, 205-208.

Ittekkot, V., Safiullah, S., Arain, R., 1986. Nature of organic matter in rivers with deep sea connections: The Ganges-Brahmaputra and Indus. The Science of the Total Environment 58, 93-107.

Jørgensen, B.B., Kasten, S., 2006. Sulfur cycling and methane oxidation. In: Schulz, H.D., Zabel, M. (Eds.), Marine Geochemistry. Springer, Berlin, pp. 271-309.

Kallweit, W., Mollenhauer, W., Zabel, M., 2012. Multi-proxy reconstruction of terrigenous input and sea-surface temperatures in the eastern Gulf of Guinea over the last 35 ka. Marine Geology 319-322, 35-46.

Kates, M., 1975. Techniques of lipodology. In: Work, T.S., E. Work, E. (Eds.), Laboratory Techniques in Biochemistry and Molecular Biology. Publisher?, pp. 269-610.

Keil, R.G., Tsamakis, E., Wolf, N., Hedges, J.I., Goni, M.A., 1997. Relationships between organic carbon preservation and mineral surface area in Amazon Fan sediments (Holes 932A and 942A). In: Flood, R.D., Piper, D.J.W., Klaus, A., L.C. Peterson, L.C. (Eds.), Proceedings of the Ocean Drilling Program, Scientific Results, 155. College Station, TX (Ocean Drilling Program), pp. 531-538.

Kim, J.-J., Talbot, H.M., Zarzycka, B., Bauersach, T., Wagner, T., 2011. Occurrence and abundance of soil-specific bacterial membrane lipid markers in the Têt watershed (Southern France): Soil-specific BHPs and branched GDGTs. Geochemistry, Geophysics, Geosystems 12 DOI: 10.1029/2010GC003364.

Kim, J.-H., Zell, C., Moreirs-Turcq, P., Pérez, M.A.P., Abril, G., Mortillaro, J.-M., Weijers, J.W.H., Meziane, T., Sinninghe Damsté, J.S., 2012. Tracing soil organic carbon in the lower Amazon River and its tributaries using GDGT distributions and bulk organic matter properties. Geochimica et Cosmochimica Acta 90, 163–180.

Kineke, G.C., Sternberg, R.W., Trowbridge, J.H., Geyer, W.R., 1996. Fluid-mud processes on the Amazon continental shelf. Continental Shelf Research 16, 667-696.

Kuehl, S.A., DeMaster, D.J., Nittrouer, C.A., 1986. Nature of sediment accumulation on the Amazon continental shelf. Continental Shelf Research, 6, 209-225.

Leider, A., Hinrichs, K.-U., Mollenhauer, G., Versteegh, G.J.M., 2010. Core-top calibration of the lipid-based UK'37 and TEX_{86} temperature proxies on the southern Italian shelf (SW Adriatic Sea, Gulf of Taranto). Earth and Planetary Science Letters 300, 112-124.

Martinelli, I.A., Pessenda, L.C.R., Espinoza, E., Camargo, P.B., Telles, F.C., Cerri, C.C., Victoria, R.L., Aravena, R., Richey, J., Trumbore, S., 1996. Carbon-13 variation with depth in soils of Brazil and climate change during the Quaternary. Oecologia 106, 376-381.

Melack, J.M., Hess, L.L., 2010. Remote sensing of the distribution and extent of wetlands in the Amazon Basin. In: Junk, W.J., Wittmann, F., Parolin, P., Piedade, M.T.F., Schöngart, J. (Eds.), Amazonian Floodplain Forests - Ecophysiology, Biodiversity, and Sustainable Management. Springer, Dordrecht, pp. 43-60.

Melack, J.M., Hess, L.L., Gastil, M., Forsberg, B.R., Hamilton, S.K., Lima, I.B.T., Novo, E., 2004. Regionalization of methane emissions in the Amazon Basin with microwave remote sensing. Global Change Biology, 10, 530-544.

Meybeck, M., Ragu, A., 1996. River discharges to the Oceans: An assessement of suspended solids, major ions and nutrients. Environment Information and Assessment Rpt. UNEP, Nairobi, 250 pp.

Milliman, J.D., Summerhayes, C.P., Barretto, H.T., 1975. Quaternary sedimentation on the Amazon continental margin: A model. Geological Society of America Bulletin, 86, 610-614.

Mollenhauer, G., Eglinton, T.I., Ohkouchi, N., Schneider, R.R., Müller, P.J., Grootes, P.M., Rullkötter, J., 2003. Asynchronous alkenone and foraminifera records from the Benguela Upwelling System. Geochimica et Cosmochimica Acta, 67, 2157-2171.

Mollenhauer, G., Schneider, R.R., Jennerjahn, T., Müller, P.J., Wefer, G., 2004). Organic carbon accumulation in the South Atlantic Ocean: its modern, mid-Holocene and last glacial distribution. Global and Planetary Change 40, 249-266.

Mollenhauer, G., Kienast, M., Lamy, F., Meggers, H., Schneider, R.R., Hayes, J.M., Eglinton, T.I., 2005. An evaluation of ^{14}C age relationships between co-occurring foraminifera, alkenones, and total organic carbon in continental margin sediments. Paleoceanography 20, PA1016, doi:10.1029/2004PA001103.

Mollenhauer, G., Schneider, R.R., Müller, P.J., Spieß, V., Wefer, G., 2002. Glacial/interglacial variablity in the Benguela upwelling system: Spatial distribution and budgets of organic carbon accumulation. Global Biogeochemical Cycles 16, 1134, doi: 10.1029/2001gb001488.

Moreira-Turcq, P., Seyler, P., Guyot, J.L., Etcheber, H., 2003. Exportation of organic carbon from the Amazon River and its main tributaries. Hydrological Processes 17, 1329–1344.

Ohkouchi, N., Eglinton, T.I., Keigwin, L.D., Hayes, J.M., 2002. Spatial and temporal offsets between proxy records in a sediment drift. Science 298, 1224-1227.

Ourisson, G., Rohmer, M., Poralla, K., 1987. Prokaryotic hopanoids and other polyterpenoid sterol surrogates. Annual Review of Microbiology 41, 301-333.

Pessenda, L.C.R., Gouveia, S.E.M., Aravena, R., 2001. Radiocarbon dating of total soil organic matter and humin fraction and its comparison with ^{14}C ages of fossil charcoal. Radiocarbon 43, 595-601.

Pessenda, L.C.R., Gouveia, S.E.M., Aravena, R., Gomes, B.M., Boulet, R., Ribeiros, A.S., 1998. ^{14}C dating and stable carbon isotopes of soil

organic matter in forest-savanna boundary areas in the southern Brazilian Amazon region. Radiocarbon 40, 1013-1022.

Pessenda, L.C.R., Gouveia, S.E.M., Ribeiro, A.d.S., De Oliveira, P.E., Aravena, R., 2010. Late Pleistocene and Holocene vegetation changes in northeastern Brazil determined from carbon isotopes and charcoal records in soils. Palaeogeography, Palaeoclimatology, Palaeoecology, 297, 597-608.

Peterse, F., Kim, J.-H., Schouten S., Klitgaard Kristensen D., Koç, N., Sinninghe Damsté, J.S., 2009. Constraints on the application of the MBT-CBT palaeothermometer at high latitude environments (Svalbard, Noprway). Organic Geochemistry 40, 692-699.

Räsänen, M.E., Salo, J.S., Jungner, H., 1991. Holocene floodplain lake sediments in the Amazon: ^{14}C dating and palaeoecological use. Quaternary Science Reviews 10, 363-372.

Raymond, P.A., Bauer, J.E., 2001. Riverine export of aged terrestrial organic matter to the North Atlantic Ocean. Nature 409, 497-500.

Reimer, P., Baillie, M., Bard, E., Bayliss, A., Beck, J., Blackwell, P., Bronk Ramsey, C., Buck, C., Burr, G., Edwards, R., Friedrich, M., Grootes, P., Guilderson, T., Hajdas, I., Heaton, T., Hogg, A., Hughen, K., Kaiser, K., Kromer, B., McCormac, F., Manning, S., Reimer, R., Richards, D., Southon, J., Talamo, S., Turney, C.S.M., van der Plicht, J., Weyhenmeyer, C.E., 2009. IntCal09 and Marine09 Radiocarbon Age Calibration Curves, 0–50,000 Years cal BP. Radiocarbon 51, 1111-1150.

Rethemeyer, J., Schubotz, F., Talbot, H.M., Cooke, M.P., Hinrichs, K.-U., Mollenhauer, G., 2010. Distribution of polar membrane lipids in permafrost soils and sediments of a small high Arctic catchment. Organic Geochemistry 41, 1130-1145.

Rohmer, M., Bouvier-Nave, P., Ourisson, G., 1984. Distribution of hopanoid triterpenes in prokaryotes. Journal of General Microbiology 130, 1137-1150.

Sáenz, J.P., Eglinton, T.I., Summons, R.E., 2011. Abundance and structural diversity of bacteriohopanepolyols in suspended particulate matter along a river to ocean transect. Organic Geochemistry 42, 774-780.

Schlünz, B., 1998. Riverine organic carbon input to the ocean in relation to Late Quaternary climate change, 116, pp. 1-136. University of Bremen, Bremen. Is this a thesis, book or what?

Schlünz, B., Schneider, R.R., 2000. Transport of terrestrial organic carbon to the oceans by rivers: re-estimating flux- and burial-rates. International Journal of Earth Sciences 88, 599-606.

Schlünz, B., Schneider, R.R., Müller, P.J., Wefer, G., 2000. Late Quaternary organic carbon accumulation south of Barbados: infuence of the Orinoco and Amazon rivers? Deep-Sea Research I 47, 1101-1124.

Schlünz, B., Schneider, R.R., Müller, P.J., Showers, W.J., Wefer, G., 1999. Terrestrial organic carbon accumulation on the Amazon deep sea fan during the last glacial sea level low stand. Chemical Geology 159, 263-281.

Schouten, S., Hopmans, E.C., van der Meer, J., Mets, A., Bard, E., Bianchi, T.S., Diefendorf, A., Escala, M., Freeman, K.H., Furukawa, Y., Huguet, C., Ingalls, A., Ménot-Combes, G., Nederbragt, A.J., Oba, M., Pearson, A., Pearson, E.J., Rosell-Melé, A., Schaeffer, P., Shah, S.R., Shanahan, T.M., Smith, R.W., Smittenberg, R., Talbot, H.M., Uchida, M., Van Mooy, B.A.S., Yamamoto, M., Zhang, Z., Sinninghe Damsté, J.S., 2009. An interlaboratory study of TEX_{86} and BIT analysis using high-performance liquid chromatography-mass spectrometry. Geochemistry Geophysics Geosystems, 10, Q03012, doi: 10.1029/2008GC002221.

Schouten, S., Hopmans, E.C., Sinninghe Damsté, J.S., 2013. The organic geochemistry of glycerol dialkyl glycerol tetraether lipids: A review. Organic Geochemistry 54, 19–61.

Schulz, H.D., Dahmke, A., Schinzel, U., Wallmann, K., Zabel, M., 1994. Early diagenetic processes, fluxes, and reaction rates in sediments of the South Atlantic. Geochimica et Cosmochimica Acta 58, 2041-2060.

Schulz H.D., Andersen N., Breitzke M., Burda D., Dehning K., Diekamp V., Felis T., Gerlach H., Gumprecht R., Hinrichs S., Petermann H., Pimenta C. C., Pototzki F., Probst U., Rode H., Sagemann J., Schinzel U., Schmidt H., Schneider R., Segl M., Showers W.J., Tegeler M. D., Thiessen W., Treppke U., Zabel M., 1991. Bericht und erste Ergebnisse über die Meteor-Fahrt M 16/2. Recife - Belem, 28.4. - 21.5.1991. Berichte, Fachbereich Geowissenschaften, Universität Bremen, Bremen, 149 pp.

Shipboard Scientific Party, 1995. Site 931. In: W.J.,Wittmann, F., Parolin, P., Piedade, M.T.F., Schöngart, J. (Eds.), Proceedings of the Ocean Drilling

Program, Initial Reports, 155. College Station, TX (Ocean Drilling Program), pp. 123-174.

Sommerfield, C.K., Nittrouer, C.A., Figueiredo, A.G., 1995. Stratigraphic evidence of changes in Amazon shelf sedimentation during the late Holocene. Marine Geology 125, 351-371.

Stuiver, M., Reimer, P.J., Reimer, R., 2010. CALIB - Radiocarbon Calibration, Version 6.0. http://calib.qub.ac.uk/calib/.

Talbot, H.M., Squier, A.H., Keely, B.J., Farrimond, P., 2003a. Atmospheric pressure chemical ionisation reversed-phase liquid chromatography/ion trap mass spectrometry of intact bacteriohopanepolyols. Rapid Communications in Mass Spectrometry 17, 728-737.

Talbot, H.M., Summons, R.E., Jahnke, L.L., Farrimond, P., 2003b. Characteristic fragmentation of bacteriohopanepolyols during atmospheric pressure chemical ionisation liquid chromatography/ion trap mass spectrometry. Rapid Communications in Mass Spectrometry 17, 2788-2796.

Talbot, H.M., Watson, D.F., Pearson, E.J., Farrimond, P., 2003c. Diverse biohopanoid compositions of non-marine sediments. Organic Geochemistry 34, 1353-1371.

Talbot, H.M., Farrimond, P., 2007. Bacterial populations recorded in diverse sedimentary biohopanoid distributions. Organic Geochemistry 38, 1212-1225.

Talbot, H.M., Rohmer, M., Farrimond, P., 2007a. Rapid structural elucidation of composite bacterial hopanoids by atmospheric pressure chemical

ionisation liquid chromatography/ion trap mass spectrometry. Rapid Communications in Mass Spectrometry 21, 880-892.

Talbot, H.M., Rohmer, M., Farrimond, P., 2007b. Structural characterisation of unsaturated bacterial hopanoids by atmospheric pressure chemical ionisation liquid chromatography/ion trap mass spectrometry. Rapid Communications in Mass Spectrometry 21, 1613-1622.

Talbot, H.M., Summons, R.E., Jahnke, L.L., Cockell, C.S., Rohmer, M., Farrimond, P., 2008. Cyanobacterial bacteriohopanepolyol signatures from cultures and natural environmental settings. Organic Geochemistry 39, 232-263.

Taylor, K.A., Harvey, H.R., 2011. Bacterial hopanoids as tracers of organic carbon sources and processing across the western Arctic continental shelf. Organic Geochemistry 42, 487–497.

van Winden, J.F., Talbot, H.M., Kip, N., Reichart, G.-J., Pol, A., McNamara, N.P., Jetten, M.S.M., Op den Camp, H.J.M., Sinninghe Damsté, J.S., 2012. Bacteriohopanepolyol signatures as markers for methanotrophic bacteria in peat moss. Geochimica et Cosmochimica Acta 77, 52-61.

Walsh, E.M., Ingalls, A.E., Keil, R.G., 2008. Sources and transport of terrestrial organic matter in Vancouver Island fjords and the Vancouver-Washington Margin: A multiproxy approach using $\delta^{13}C_{org}$, lignin phenols, and the ether lipid BIT index. Limnology and Oceanography 53, 1054-1063.

Weijers, J.W.H., Schouten, S., Schefuß, E., Schneider, R.R., Sinninghe Damsté, J.S., 2009. Disentangling marine, soil and plant organic carbon

contributions to continental margin sediments: A multi-proxy approach in a 20,000 year sediment record from the Congo deep-sea fan. Geochimica et Cosmochimica Acta 73, 119-132.

Weijers, J.W.H., Schouten, S., Spaargaren, O.C., Sinninghe Damsté, J.S., 2006. Occurrence and distribution of tetraether membrane lipids in soils: Implications for the use of the TEX_{86} proxy and the BIT index. Organic Geochemistry 37, 1680-1693.

Weijers, J.W.H., Schouten, S., van den Donker, J.C., Hopmans, E.C., Sinninghe Damsté, J.S., 2007. Environmental controls on bacterial tetraether membrane lipid distribution in soils. Geochimica et Cosmochimica Acta 71, 703-713.

Wilson, K.E., M.A., M., Burns, S.J., 2011. Evidence for a prolonged retroflection of the North Brazil Current during glacial stages. Palaeogeography, Palaeoclimatology, Palaeoecology 301, 86-96.

Xu, Y., Cooke, M.P., Talbot, H.M., Simpson, M.E., 2009. Bacteriohopanepolyol Signatures of Bacterial Populations in Western Canadian Soils. Organic Geochemistry 40, 79-86.

Zell, C., Kim, J.-H., Moreirs-Turcq, P., Abril, G., Hopmans, E.C., Bonnet, M.-P., Lima Sobrinho, R., Sinninghe Damsté, J.S., 2013. Disentangling the origins of branched tetraether lipids and crenarchaeol in the lower Amazon River: Implications for GDGT-based proxies. Limnology and Oceanography 58, 343–353.

Zhu, C., Weijers, J.W.H., Wagner, T., Pan, J.-M., Chen, J.-F., Pancost, R.D., 2011a. Sources and distributions of tetraether lipids in surface sediments

across a large river-dominated continental margin. Organic Geochemistry 42, 376–386.

Zhu, C., Talbot, H.M., Wagner, T., Pan, J.-M., Pancost, R.D., 2011b. Distribution of hopanoids along a land to sea transect: implications for microbial ecology and the use of hopanoids in environmental studies. Limnology and Oceanography 56, 1850-1865.

Zhu, C., Wagner, T., Talbot, H.M., Weijers, J.W.H., Pan, J.-M., Pancost, R.D., 2013. Mechanistic controls on diverse fates of terrestrial organic components in the East China Sea. Geochimica et Cosmochimica Acta 117, 129-143.

Figure captions

Fig. 1. (a) Map of sampling locations of gravity cores and (b) of wetland locations in the interior of the Amazon catchment near the Colombian town of Puerto Nariño.

Fig. 2. Downcore profiles of TOC, BIT, R_{soil} and concentration of total, soil marker and methane oxidation (CH_4 ox) BHP markers for GeoB3918 (top) and GeoB1514 (bottom).

Fig. 3. Relative contribution of main BHP groups of all BHPs in cores (a) GeoB3918 and (b) GeoB1514. Main groups are divided into BHPs specific for aerobic methane oxidation (i.e "CH_4 ox"; **Id**, **Ic**, **Ic'** and **III** or **IVc**), aminotriol (**Ie**), soil-marker BHPs (**Ia**, **IIa**, **Ib**, **IIb**, **Ib'**, **IIb')** and all other BHPs.

Fig. 4. Relative contribution of main BHP groups of all BHPs in sediment and soil samples from the Puerto Nariño region. Main groups are divided into BHPs specific for aerobic methane oxidation (i.e "CH_4 ox"; **Id**, **Ic**, **Ic'** and **III** or **IVc**), aminotriol (**Ie**), soil marker BHPs (**Ia**, **IIa**, **Ib**, **IIb**, **Ib'**, **IIb')** and all other-BHPs.

Fig. 5. MBT/CBT age/depth correlation of GeoB1514 based on data from ODP 942 (after Bendel et al., 2009).

Fig. 6. Scatter plot comparing BIT and R_{soil} data from GeoB3918 and GeoB1514.

Appendix 1.

Ring system and side chains of selected BHPs observed sediment and soil samples. All side chain structures shown have previously been unambiguously identified from NMR. When assigned here using LC-MS only, where stereochemistry cannot be confirmed, we have assumed the structure to be the same as that previously characterized but the occurrence of additional/alternative isomers cannot be excluded. Side chain structures **b** and **b'** are based on LC-MS^n analysis only and are distinguished by the presence of ions in the APCI MS^2 spectrum of m/z 151 for **b** and m/z 192 for **b´**.

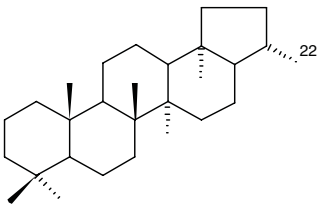

I

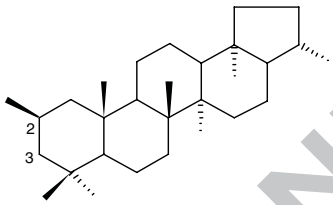

II

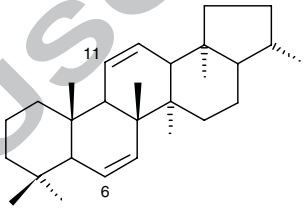

III: Δ^6; IV: Δ^{11}

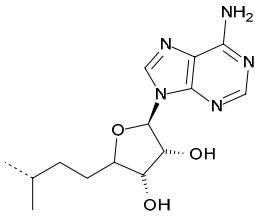

a

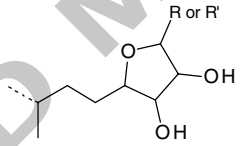

b, b´

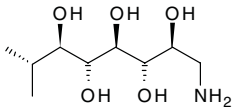

c

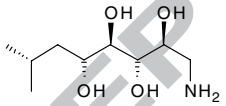

d

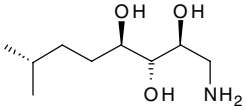

e

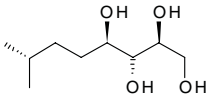

f

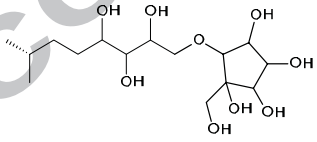

g

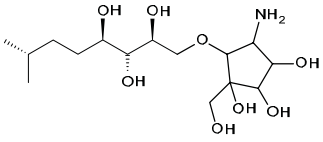

h

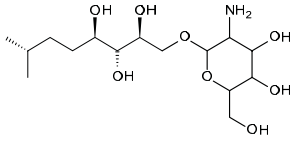

i

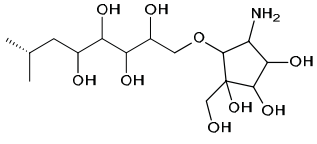

j

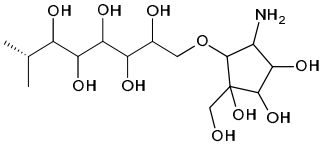

k

Table 1. BHPs listed by trivial name, structure number (see Appendix), identifying characteristic APCI base peak ion (*m/z*), known source organisms and/or environment and supporting reference.

Trivial name	Structure	APCI base peak ion m/z	Source organisms and/or typical associated settings	Reference
Adenosylhopane	**Ia**	746+788+830	N-fixing bacteria/soils	Talbot et al., 2007a
2-Methyladenosylhopane	**IIa**	760+802+844	N-fixing bacteria/soils	Talbot et al., 2007a
"Soil marker group 2"	**Ib**	761	N-fixing bacteria/soils	Cooke et al., 2008a
2-Methyl "soil-marker group 2"	**IIb**	775	soils	Cooke et al., 2008a
soil-marker group 3	**Ib'**	802	soils	Rethemeyer et al., 2010
2-Methyl "soil-marker group 3"	**IIb'**	816	soils	Rethemeyer et al., 2010
Aminopentol	**Ic**	830	Type I methanotrophs (and 1 *Desulfovibrio* sp.)	van Winden et al., 2012
Aminopentol (early isomer)	**Ic'**	788	Type I methanotrophs	van Winden et al., 2012
unsaturated aminopentol	**IIIc/IVc**	828	Type I methanotrophs	van Winden et al., 2012
aminotetrol	**Id**	772	Methanotrophs (and some *Desulfovibrio* sp.)	van Winden et al., 2012
Aminotriol	**Ie**	714	Various including methanotrophs and some *Desulfovibrio* sp.	van Winden et al., 2012
unsaturated aminotriol	**IIIe/IVe***	712	Type I methanotroph	van Winden et al., 2012
2-Methylaminotriol	**IIe**	728	cyanobacteria	Talbot et al., 2008
BHT	**If**	655	Various	Talbot and Farrimond, 2007
BHT isomer	**If'**	655	Unknown/anoxic water columns and underlying sediment	Sáenz et al., 2011

2-Methyl BHT	**IIf**	669	Cyanobacteria, *R. palustris*	Talbot et al., 2008
unsaturated BHT-pseudopentose	**IIIg/IVg**	941/983	Cyanobacteria	Talbot et al., 2008
BHT-pseudopentose	**Ig**	943/985	Cyanobacteria	Talbot et al., 2008
BHT-cyclitol ether	**Ih**	1002/1044	Various	Talbot et al., 2008
BHT-glucosamine	**Ii**	1002	Various	Talbot et al., 2008
2-MethylBHT-cyclitol ether	**IIh**	1016	Cyanobacteria	Talbot et al., 2008
Bhpentol-cyclitol ether	**Ij**	1060/1102	Various	Talbot et al., 2008
Bhhexol-cyclitol ether	**Ik**	1118/1160	Unknown/soils, peat and sediments	Talbot et al., 2008
2-MethylBHhexol-cyclitol ether	**IIk**	1132	Unknown/soils	Cooke et al., 2008a

*Alternative structure may include unsaturation in the side chain (see van Winden et al., 2012).

Table 2

Location, concentration of BHPs µg.g$^{-1}_{TOC}$ (normal text) and relative % (italics)_of BHPs in Amazon catchment samples from 6 sites

					soil markers					CH_4 ox				aminotriol			other BHPs									
Site	**Location**	**Description**	**Depth (cm)**	**TOC (%)**	**Ia**	**IIa**	**Ib**	**IIb**	**Ib'**	**Id**	**IIIc/ IVc**	**Ic**	**Ic'**	**Ie**	**IIIe/ IVe**	**IIe**	**If**	**If'**	**IIf**	**IIIg/ IVg**	**Ig**	**Ih**	**IIh**	**Ii**	**Ij**	**Ik**	**IIk**
1	3°47'5.04"S	Wetland	0-10	5.61	68[a]	12	5.6	2.3	4.4	32	13	150		150			43	7.8	9.8			250	21	4	42	9.4	0.9
	70°22'56.81"W	sediment			*8.2*[b]	*1.5*	*0.7*	*0.3*	*0.5*	*3.9*	*1.6*	*18.2*		*18.2*			*5.2*	*0.9*	*1.2*			*30.3*	*2.5*	*0.5*	*5.1*	*1.1*	*0.1*
			200-250	1.66	17					66	17	210		210	19	6.5	29	10				53	5.4	3.6	5.1	3.6	
					2.6					*10.1*	*2.6*	*32.1*		*32.1*	*2.9*	*1*	*4.4*	*1.5*				*8.1*	*0.8*	*0.5*	*0.8*	*0.5*	
2	3°48'12.24"S	Wetland	0-10	0.73	31					48	16	170		170	13	5	31					53	5	2.2	8	6.4	
	70°25'7.51"W	sediment			*5.5*					*8.6*	*2.9*	*30.4*		*30.4*	*2.3*	*0.9*	*5.5*					*9.5*	*0.9*	*0.4*	*1.4*	*1.1*	
			25-30	1.95	120		15			380	120	790		660	66		180				17	510	17	12	44	16	3
					4.1		*0.5*			*12.9*	*4.1*	*26.8*		*22.4*	*2.2*		*6.1*				*0.6*	*17.3*	*0.6*	*0.4*	*1.5*	*0.5*	*0.1*
3	3°45'18.68"S	Wetland	0-25	18.08	12	4.6	1.4			15	7.1	55	7.3	41	1.8		49	7.8				60	4.1	1.3	9.1	9.1	1.1
	70°30'40.59"W	sediment			*4.2*	*1.6*	*0.5*			*5.2*	*2.5*	*19.2*	*2.5*	*14.3*	*0.6*		*17.1*	*2.7*				*20.9*	*1.4*	*0.5*	*3.2*	*3.2*	*0.4*
4	3°39'17.68"S	Ox-bow lLake	0-10	2.35	120	17	19	4.6		5.2	1.8	37		53	11	2.2	47		12	28	22	180	6.1	6.1	11	13	2.1
	70°35'39.03"W	sediment			*20.1*	*2.8*	*3.2*	*0.8*		*0.9*	*0.3*	*6.2*		*8.9*	*1.8*	*0.4*	*7.9*		*2*	*4.7*	*3.7*	*30.1*	*1*	*1*	*1.8*	*2.2*	*0.4*
			50-75	0.23	46	4.7	6.3			2.7	2.7	11		26	2.7		31	7.7	8.4		51	99	7.8	10	4.9	4.1	
					14.1	*1.4*	*1.9*			*0.8*	*0.8*	*3.4*		*8*	*0.8*		*9.5*	*2.4*	*2.6*		*15.6*	*30.4*	*2.4*	*3.1*	*1.5*	*1.3*	
5	3°51'40.31"S	Seasonally	Oct-20	0.71	130	19	52			21		67		130			260		31			360			35	32	
	70°13'56.82"W	innundated soil			*11.4*	*1.7*	*4.6*			*1.8*		*5.9*		*11.4*			*22.9*		*2.7*			*31.7*			*3.1*	*2.8*	
6	3°47'26.78"S	Terra firme	Oct-20	1.62	130	6.6	56	33		7.7				50	4.8		43		29			390			31	33	2.2
	70°17'37.72"W	soil			*15.9*	*0.8*	*6.9*	*4*		*0.9*				*6.1*	*0.6*		*5.3*		*3.6*			*47.8*			*3.8*	*4*	*0.3*

Table 3. ^{14}C age and $\delta^{13}C$ value for samples from GeoB3918 and GeoB1514 [note that TOC ^{14}C ages were calibrated (see methods for further details)].

Core	Depth (m)	$\delta^{13}C$ (‰)	^{14}C age (yr BP)	Age error (yr)	Material	Cal. Age (yr BP)	Cal. Age error (yr)
GeoB3918	3.84		860	40	Bivalve	450	40
GeoB3918	4.49		1030	40	Bivalve	580	40
GeoB3918	0.30 - 0.36	-25.67	3740	35	TOC		
GeoB3918	2.30 - 2.36	-25.64	4050	35	TOC		
GeoB3918	4.50 - 4.56	-25.31	3910	35	TOC		
GeoB1514	0.40 - 0.50	-23.86	13650	75	TOC		
GeoB1514	2.22 - 2.32	-24.60	19500	100	TOC		
GeoB1514	4.22 - 4.32	-24.85	23100	160	TOC		
GeoB1514	6.80 - 6.90	-26.89	30200	180	TOC		

Table 4. GeoB3918 (left) and GeoB1514 (right) TOC (%), concentration (µg/g TOC) of brGDGTs and crenarchaeol and calculated BIT and R_{soil} index values.

GeoB 3918						GeoB 1514					
Depth	TOC (%)	Br-GDGTs	Cren	BIT	R_{soil}	Depth	TOC (%)	Br-GDGTs	Cren	BIT	R_{soil}
(cm)						**(cm)**					
3	0.66	53.6	47.2	0.53	0.21	10	0.3	10.4	14.3	0.53	0.00
12	0.59	49	29.5	0.62	0.23	28	0.29	9.6	6.5	0.67	0.05
29	0.70	54.4	26.3	0.67	0.2	45	0.5	71.3	77.6	0.50	0.06
47	0.62	52.8	29.1	0.64	0.25	75	0.53	174.9	35	0.83	0.16
67	0.65	43.2	24.3	0.64	0.24	105	0.57	210.9	50.6	0.80	0.25
89	0.59	50.6	41.5	0.55	0.24	130	0.57	199.5	31.4	0.86	0.15
109	0.70	68.6	35.3	0.66	0.27	155	0.68	194.3	30.4	0.86	0.39
129	0.64	54.6	48.2	0.53	0.24	180	0.61	175.8	36.2	0.82	0.15
149	0.62	64.4	27.1	0.7	0.22	205	0.58	196.5	47.8	0.80	0.21
169	0.64	56.8	35.3	0.62	0.25	232	0.54	202.5	28.9	0.87	0.23
189	0.63	54.6	44.3	0.55	0.25	255	0.58	174.9	73	0.70	0.27
209	0.63	60.5	40.3	0.6	0.26	280	0.54	131.7	39.6	0.77	0.09
249	0.62	68.4	33.8	0.67	0.25	305	0.56	162.4	30.7	0.83	0.20
269	0.66	61	27	0.69	0.29	330	0.62	183.6	50.3	0.78	0.09
289	0.65	50.8	44.2	0.53	0.26	355	0.54	181.8	40.2	0.81	0.05
309	0.67	57.2	28.1	0.67	0.29	380	0.63	224.6	74.3	0.75	0.20
329	0.60	59	27.7	0.68	0.27	405	0.57	231.2	69.5	0.76	0.23
349	0.72	49.9	28.2	0.64	0.26	430	0.57	199.1	41.8	0.82	0.04
369	0.64	54.9	52.6	0.51	0.28	455	0.58	198.4	45.7	0.81	0.07
389	0.6	64	33.8	0.6	0.2	480	0.5	175.6	61.	0.7	0.1

	1			5	7		6		2	4	1
409	0.64	63	39.6	0.61	0.28	505	0.64	151.8	28.2	0.84	0.31
429	0.66	51.4	49.2	0.51	0.29	530	0.78	239.4	36.7	0.86	0.23
449	0.64	52.1	39.7	0.57	0.31	555	0.78	177.6	21.4	0.88	0.13
469	0.63	65.8	37.4	0.64	0.28	580	0.89	291	42.9	0.87	0.28
489	0.67	56.6	31	0.65	0.28	605	0.88	258.6	43.2	0.85	0.14
503	0.68	65.9	36.9	0.64	0.26	630	0.74	327.9	28.3	0.91	0.19
						643	0.89	243.7	18.8	0.92	0.28
						670	0.94	211.5	23.9	0.89	0.21
						695	0.86	191.1	20.3	0.9	0.08
						708	1.00	250	29.2	0.89	0.09

Table 5. Concentration (ug/g TOC) of individual BHPs in deep sea fan core GeoB1514.

	Soil markers						CH_4 ox.				Aminotriol		Other BHPs								
Depth (cm)	Ia	IIa	Ib	IIb	Ib'	IIb'	Id	IIIc / IVc	Ic	Ic'	Ie	IIIe / IVe	If	IIf	Ig	IIg	Ih	Ij	Ik	Im	In	Total BHPs (ug/gTOC)
Holocene																						
10							6.3		19		16		61								6.1	108
28	5.9		2.5		1.8		5.9		15		18	2.5	200	24			4.5	2.4	1.6	5.1	24	303
mean Rel %	*1.4*		*0.6*		*0.4*		*3.0*		*8.3*		*8.3*	*0.6*	*63.4*	*5.8*			*1.1*	*0.6*	*0.4*	*1.2*	*7.3*	
Last Glacial																						
45			3.8				13	2.0	38	8.1	35	3.2	65	2.7			19	2.4	5.5	7.4	29	230
75	18	3.6	10		3.1	1.8	41	13	160	10	140	7.7	190	5.6			99	18	15	22	22	743
105	27		5.1				17	6.8	88	7.8	92	4.6	98	2.3			72	11	13	16	13	442
130	23	2.3	9.6		2.1	2.6	47	13	120	6.5	320	7.9	220	9.6	11		93	15	16	23	28	930
155	120	6.5	28	4.6	2.8		33	11	120	15	320	30	250	9.9			250	27	14	20	56	1156
180	57	7.4	28	3.5			31	6.9	140	14	340	14	550	23	26		230	31	24	25	97	1552
205	14	2.9	11	4.2	2.2	2.2	11	4.4	49	4.3	84	4.6	140	5.2			43	11	8.6	12	66	443
232	24	4.1	14		2.2		31	6.5	81	11	160	7.2	150	5.2	11		96	11	6.6	13	37	627

255	64	12	18				24	8.2	100	24	170	9.6	250	11			160	25	12	14	80	888
280	13		3.8				14	2.7	54	4.5	100	5.5	170	5.7	14	4.6	64	7.1	9.3	18	37	510
305	28		14			1.5	25	7.1	100	8.7	120	13	170	5.9			97	14	21	10	31	623
330	21		10				48		190	9.8	290	10	320	12			410	52	42	24	76	1484
355	18						24	3.4	93	15	160	12	330	11	18	5.3	140	19	15	16	66	928
380	34	6.3	15				19	3.3	65	11	140	9.3	220	5.9			85	13	6.5	10	58	646
405	56	7.6	12		2.2	1.8	53	11	200	5.5	300	14	270	21			230	44	24	13	66	1252
430	5.5		6.6				43	8.0	130	11	330	16	330	8.5	16		150	20	13	20	81	1177
455	4.5			2.9	9.9	1.1	9.5	2.0	29	3.5	73	4.8	250	8.7	16		30	4.9	2.3	28	55	517
480	33		6.4				31	8.8	140	11	230	16	330	7.4			150	14	12	23	80	1053
505	58	6.0	20		0.8	1.6	35	12	180	14	160	17	190	8.0	8.8		140	18	8.0	12	40	843
530	44		14	1.5		3.0	40	12	150	30	240	18	210	17	8.1		160	22	12	19	46	984
555	51	6.2	8.4		1.7		63	18	160	38	450	43	440	17	30		340	33	23	19	59	1733
580	55	9.7	19	3.3			24	14	160	14	260	20	220	7.6	23		170	23	26	15	39	1016
605	23		13	4.4			45	11	120	23	350	22	240	14	19		200	24	12	15	35	1130
630	120	30	14				58	20	190	26	510	24	710	49	41		470	41	34	46	130	2349
643	110	12	28		13	3.2	81	19	250	31	620	33	420	31	30		300	36	18	45	68	1982
670	46	2.	11		5.	1.	36	5.9	150	42	210	7.1	250	13			160	21	18	36	38	987

		0			4	8																
695	31						36	6.0	100	19	250	12	370	23	24		250	38	17	19	58	1222
708	20	4.4	5.2		1.0		38	8.1	130	16	240	15	300	12			190	14	11	18	29	1021
mean Rel.%	*3.5*	*0.3*	*1.2*	*0.1*	*0.2*	*0.1*	*3.3*	*0.8*	*12.1*	*1.5*	*21.3*	*1.3*	*26.1*	*1.1*	*0.9*	*0.1*	*14.8*	*2.0*	*1.5*	*2.1*	*5.6*	
SD.	*2.0*						*1.0*	*0.4*	*3.6*	*0.8*	*4.5*	*0.5*	*6.2*	*0.4*			*4.2*	*0.6*	*0.7*	*0.9*	*2.9*	

ACCEPTED MANUSCRIPT

Table 6. Concentration (ug/g TOC) of individual BHPs in shelf core GeoB3918.

	Soil markers					CH_4 ox				Aminotriol		Other BHPs							
Depth (cm)	Ia	IIa	Ib	Ib'	IIb'	Id	IIIc/ IVc	Ic	Ic'	Ie	IIIe/ IVe	If	IIf	Im	In	Ih	Ij	Ik	Total BHPs (ug/g TOC)
3	56	6.3	9.1	19	5.8	57	12	230	45	150	13	370	17	29	42	71	7.3	7.8	1147
12	47	5.9	6.7	15	2.4	89	20	360	69	230	13	260	5.1	23	21	71	9.5	8.9	1257
29	53	4.2	6.4	13	2.9	70	13	350	24	210	11	320	9.1	28	36	68	10	9.2	1238
47	76	10	13	17	4.0	42	11	240	38	140	10	360	9.8	29	42	66	5.9	10	1124
67	98	9.3	14	24		190	41	750	4.3	590	22	470	14	39	53	140	23	18	2500
89	58	5.9	8.7	18	3.4	79	19	400	22	240	18	290	6.9	32	37	78	11	13	1340
109	100	14	13	20	6.2	180	39	760	38	520	22	410	17	51	48	150	24	19	2431
129	79	10	12	16	4.6	82	16	300	88	200	18	390	13	38	47	84	12	8.6	1418
149	61	5.1	4.0	21	1.9	110	22	360	56	310	14	330	8.5	27	36	92	13	10	1482
169	110	9.2	22	34	8.6	210	40	790	44	600	26	540	15	52	62	140	21	20	2744
189	85	9.2	13	23	4.9	130	22	510	14	310	16	410	9.8	30	56	86	11	12	1752
209	110	11	20	31	4.7	110	22	540	49	310	23	490	12	47	46	130	18	16	1990
249	68	4.1	9.2	17	3.8	120	28	550	34	380	22	310	13	29	41	100	13	16	1758
269	150	14	5.4	40	10	220	48	770		660	38	530	15	49	79	190	22	23	2863
289	83	13	12	23		96	18	400	17	300	23	380	12	36	52	92	10	10	1577
309	110	12	20	41	4.9	150	36	550	20	440	30	470	12	36	53	120	15	14	2134
329	67	8.8	7.6	25	2.4	110	31	540	29	290	21	300	9.1	39	37	99	16	16	1648
349	120	15	17	34	8.4	200	21	430	83	520	36	560	19	35	74	160	17	13	2362
369	94	12	18	33	8.2	110	28	530	22	290	24	430	1.5	37	64	120	15	15	1852
389	98	14	24	34	4.2	120	23	420	16	380	23	470	16	31	60	110	10	11	1864
409	140	8.4	19	39	7.7	180	29	610	15	520	22	550	16	41	89	160	21	11	2478
429	99	12	15	26	2.8	83	17	340	69	210	17	380	11	33	67	84	14	7.4	1487
449	84	5.1	11	30	4.5	75	15	340	15	180	12	300	14	34	51	83	14	12	1280
469	110	12	16	43	8.2	150	26	530		450	18	480	16	33	70	150	11	14	2137
489	140	11	13	48	9.7	160	27	500	8.8	460	27	560	12	28	83	130	20	11	2249

503	120	12	10	46	6.3	180	41	760	8.0	530	23	560	14	52	70	150	19	14	2615
mean Rel.%	*5.0*	*0.5*	*0.7*	*1.5*	*0.3*	*6.6*	*1.3*	*26.2*	*2.0*	*18.6*	*1.1*	*23.0*	*0.7*	*2.0*	*3.0*	*6.0*	*0.8*	*0.7*	
SD.	*0.9*	*0.2*	*0.3*	*0.4*	*0.1*	*1.0*	*0.3*	*3.8*	*1.7*	*3.3*	*0.2*	*3.8*	*0.3*	*0.4*	*0.7*	*0.5*	*0.1*	*0.1*	

Highlights

- Reworked and old OC from Amazonia contributes to shelf and deep fan sediments.
- High BIT and soil-marker BHP concentration indicate persistent burial of soil OC.
- Remarkably high abundance of BHP markers for aerobic methane oxidation in marine sediments.
- Marine BHP composition is strikingly similar to those from Amazonian wetlands.
- OC from wetlands may be the primary source of marine sediment biomarkers.

Figure 1

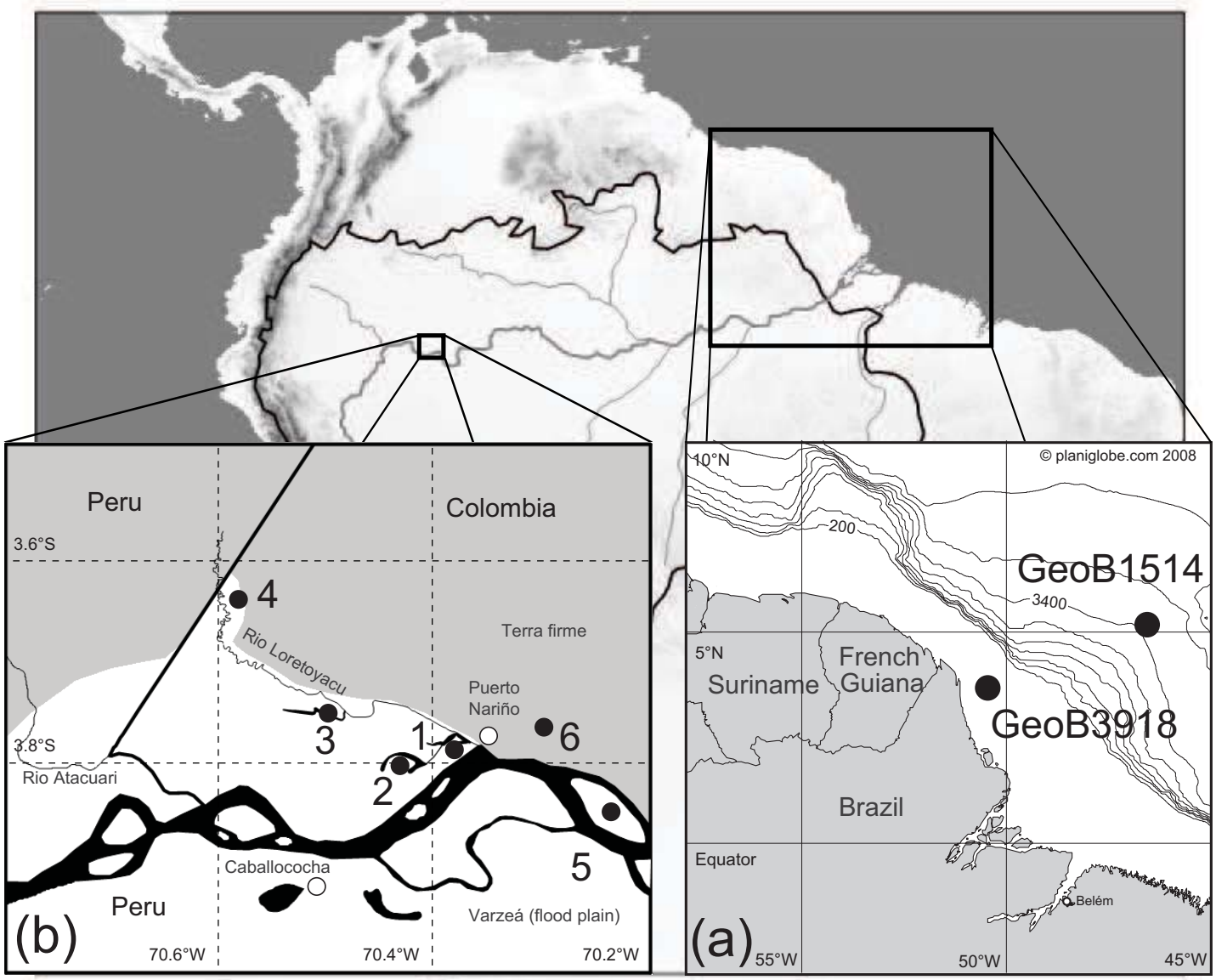

Figure 2

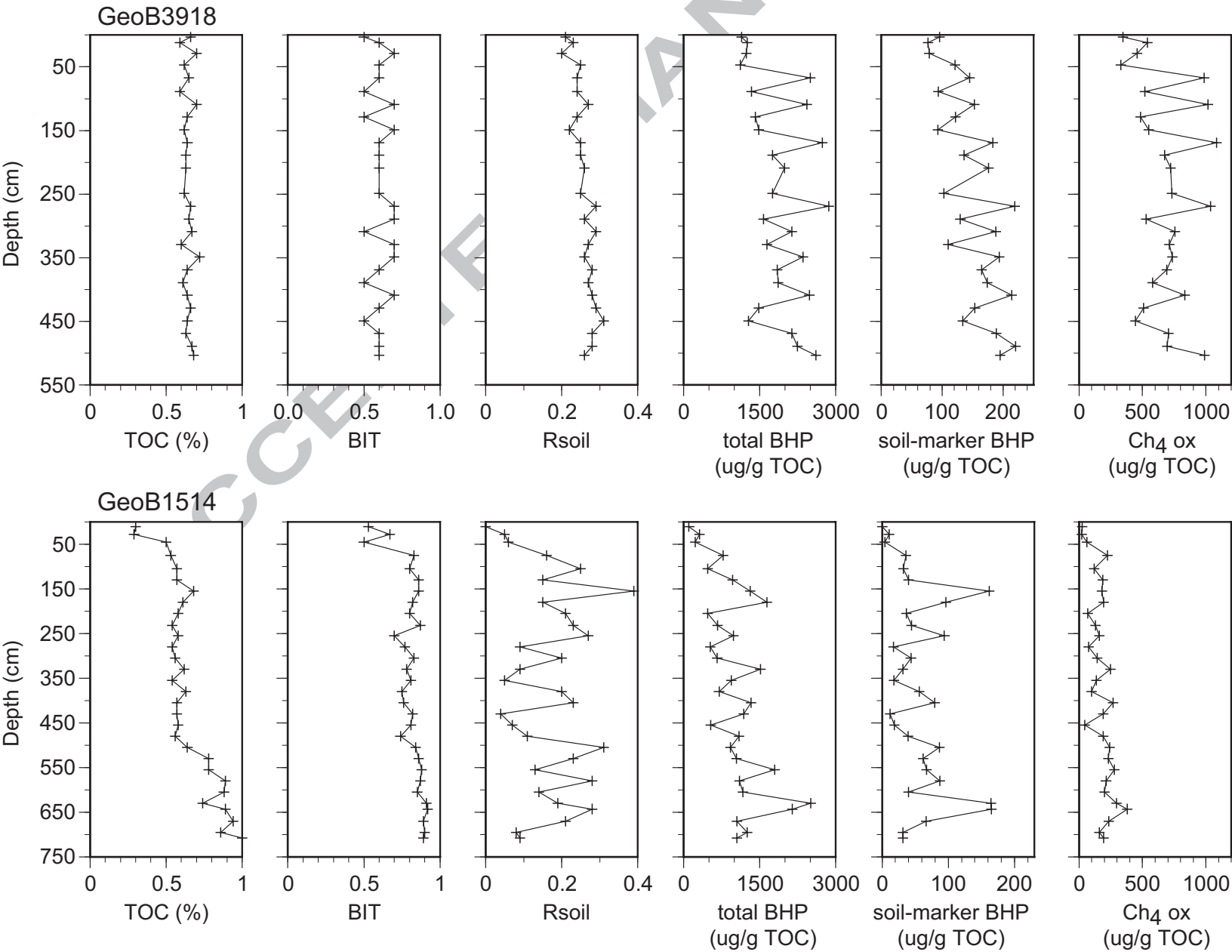

Figure 3

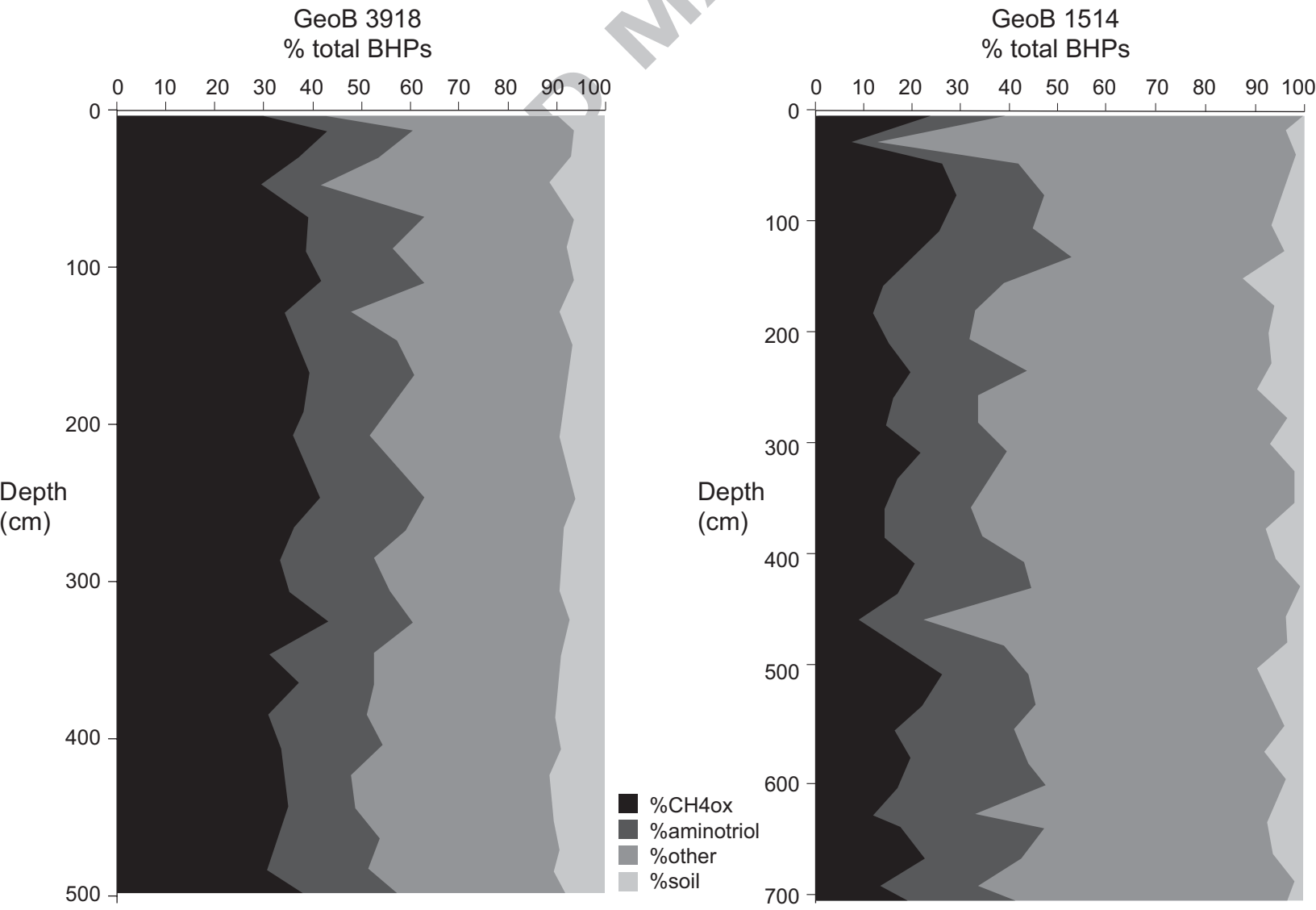

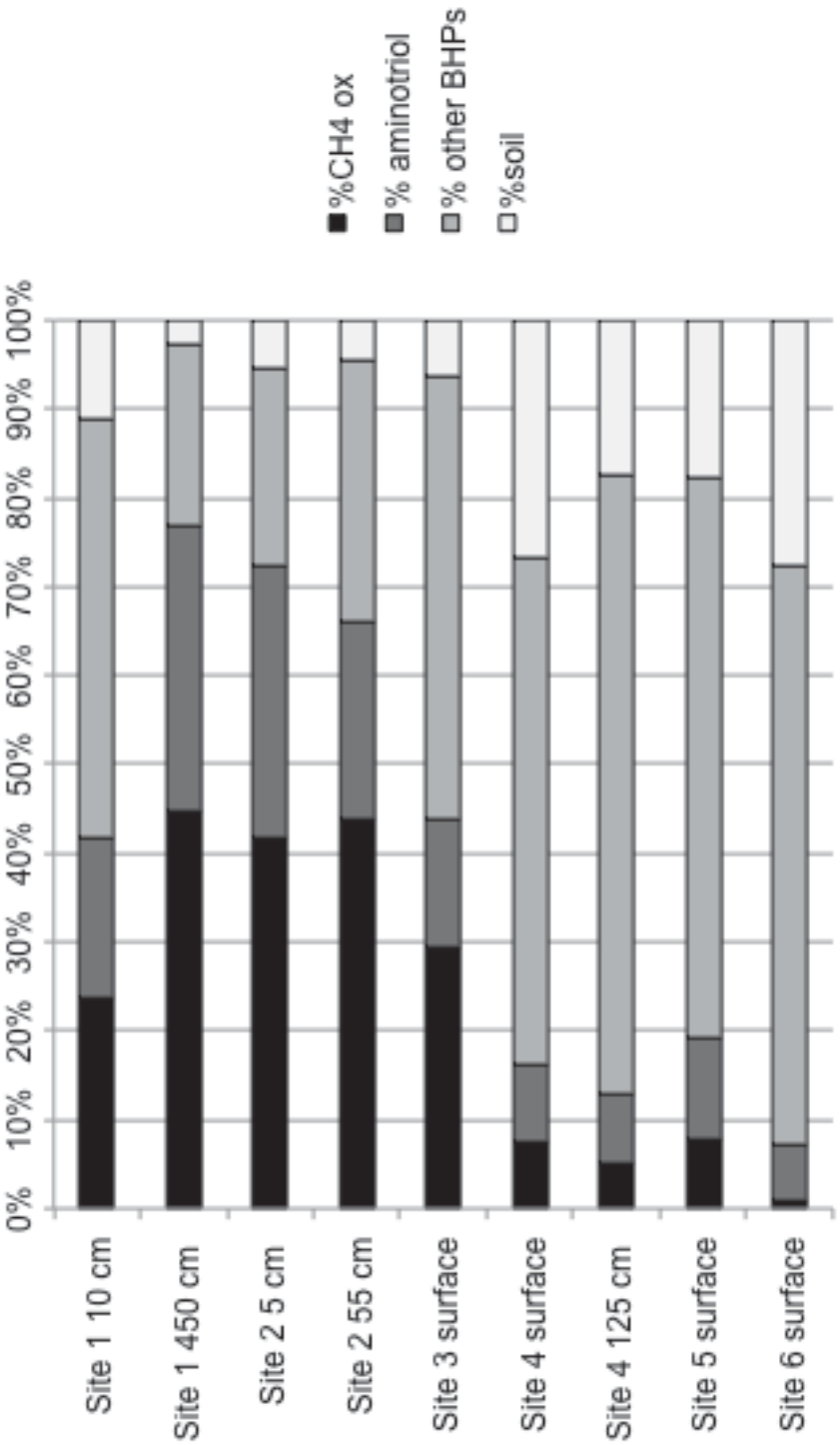

Figure 4

Figure 5

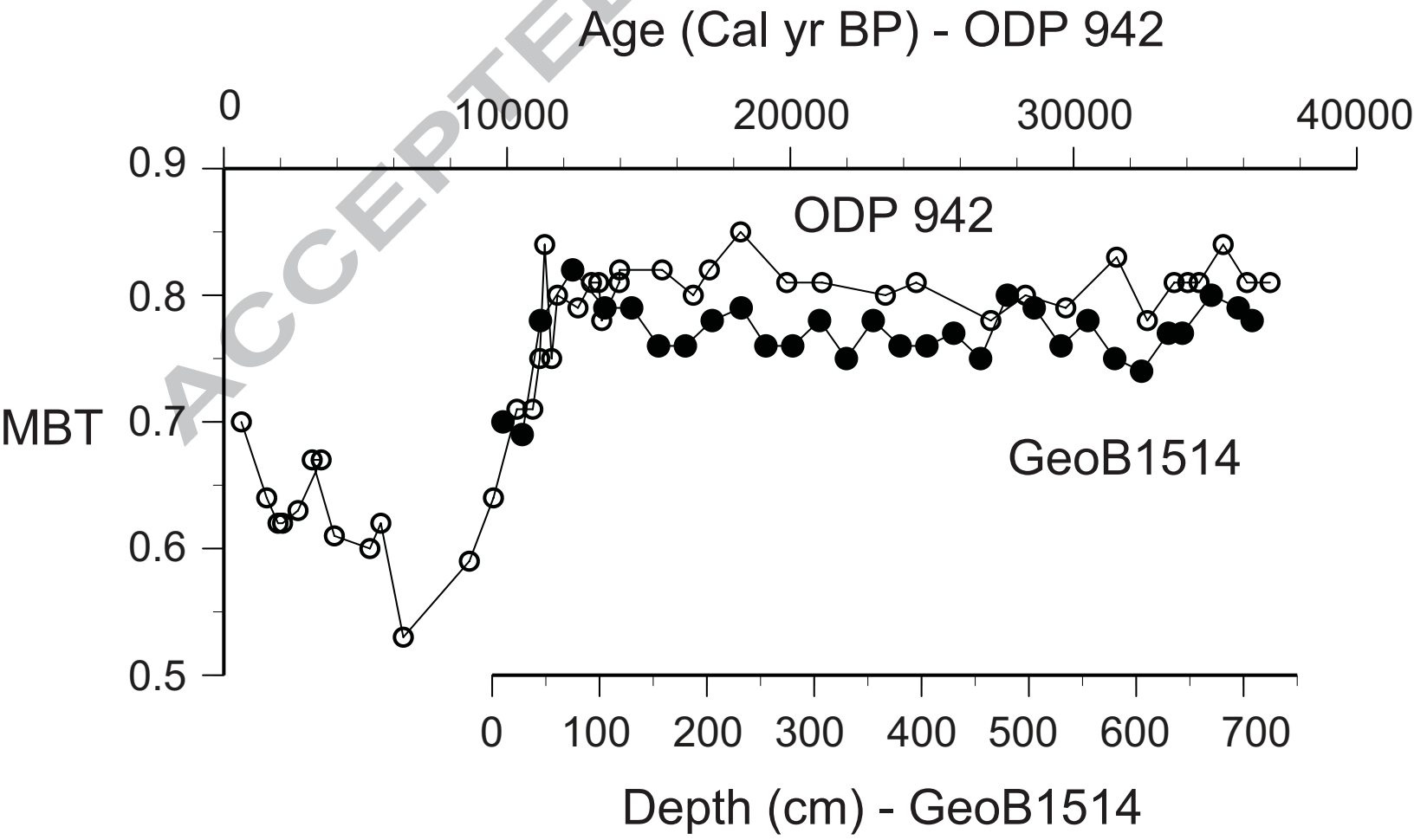

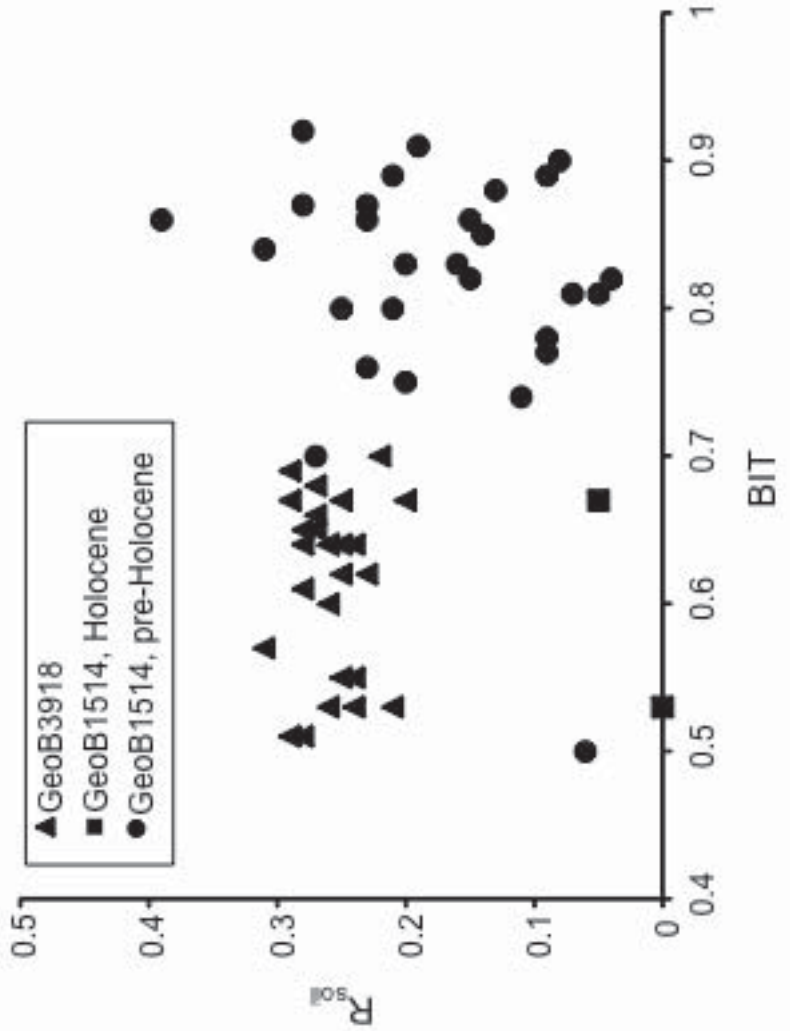

Figure 6